TISSUE ENGINEERING: Part B
Volume 15, Number 2, 2009

DOI: 10.1089/ten.teb.2008.0652

Engineering on the Straight and Narrow: The Mechanics of Nanofibrous Assemblies for Fiber-Reinforced Tissue Regeneration

Robert L. Mauck, Ph.D.,[1,2] Brendon M. Baker, B.S.,[1,2] Nandan L. Nerurkar, M.S.,[1,3]
Jason A. Burdick, Ph.D.,[2] Wan-Ju Li, Ph.D.,[4] Rocky S. Tuan, Ph.D.,[5] and Dawn M. Elliott, Ph.D.[1,2]

Tissue engineering of fibrous tissues of the musculoskeletal system represents a considerable challenge because of the complex architecture and mechanical properties of the component structures. Natural healing processes in these dense tissues are limited as a result of the mechanically challenging environment of the damaged tissue and the hypocellularity and avascular nature of the extracellular matrix. When healing does occur, the ordered structure of the native tissue is replaced with a disorganized fibrous scar with inferior mechanical properties, engendering sites that are prone to re-injury. To address the engineering of such tissues, we and others have adopted a structurally motivated approach based on organized nanofibrous assemblies. These scaffolds are composed of ultrafine polymeric fibers that can be fabricated in such a way to recreate the structural anisotropy typical of fiber-reinforced tissues. This straight-and-narrow topography not only provides tailored mechanical properties, but also serves as a 3D biomimetic micropattern for directed tissue formation. This review describes the underlying technology of nanofiber production and focuses specifically on the mechanical evaluation and theoretical modeling of these structures as it relates to native tissue structure and function. Applying the same mechanical framework for understanding native and engineered fiber-reinforced tissues provides a functional method for evaluating the utility and maturation of these unique engineered constructs. We further describe several case examples where these principles have been put to test, and discuss the remaining challenges and opportunities in forwarding this technology toward clinical implementation.

Introduction

Fiber-reinforced tissues: structure and function in health and disease

Fibrous tissues of the musculoskeletal system are dense connective tissues that serve critical load-bearing roles. The fibrous architecture of these tissues is organized to optimize this mechanical functionality. For example, tendons, ligaments, the knee menisci, and the annulus fibrosus (AF) of the intervertebral disc all transmit tensile loads generated with physiologic motion through their aligned extracellular matrix (ECM).[1–4] This ECM is most commonly comprised of collagen assembled in a hierarchical fashion into dense bundles (Fig. 1). In tissues that operate primarily in one direction, such as tendons and some ligaments, collagen is organized along the prevailing line of action, and imbues such tissues with mechanical properties that are highly anisotropic (direction dependent) and highest in the prevailing fiber orientation. In structures that experience more complicated loading patterns, such as the anterior cruciate ligament (ACL), the knee meniscus, and the AF, collagen alignment changes as a function of position within the tissue (either continuously or within discrete bundles or layers). In the AF, which experiences multiaxial tension, compression, and shear, collagen fibers in adjacent lamellae alternate between $+30$ and -30 degrees with respect to the circumference, resulting in a more complex reinforced composite (Fig. 1, center). In the meniscus, which is exposed to a similarly complicated loading environment, the majority of collagen fibers are circumferentially organized, ranging from horn insertion site to horn insertion site, with radial tie fibers interspersed and oriented perpendicular to these prevailing fiber bundles and serving to bind the tissue together. These tissues have common developmental antecedents, in that this ordered structure arises very

[1]McKay Orthopaedic Research Laboratory, Department of Orthopaedic Surgery, University of Pennsylvania, Philadelphia, Pennsylvania.
Departments of [2]Bioengineering and [3]Mechanical Engineering, University of Pennsylvania Philadelphia, Pennsylvania.
[4]Department of Orthopaedics and Rehabilitation and Biomedical Engineering, University of Wisconsin–Madison, Madison, Wisconsin.
[5]Department of Health and Human Services, Cartilage Biology and Orthopaedics Branch, National Institute of Musculoskeletal and Skin Disorders, National Institutes of Health, Bethesda, Maryland.

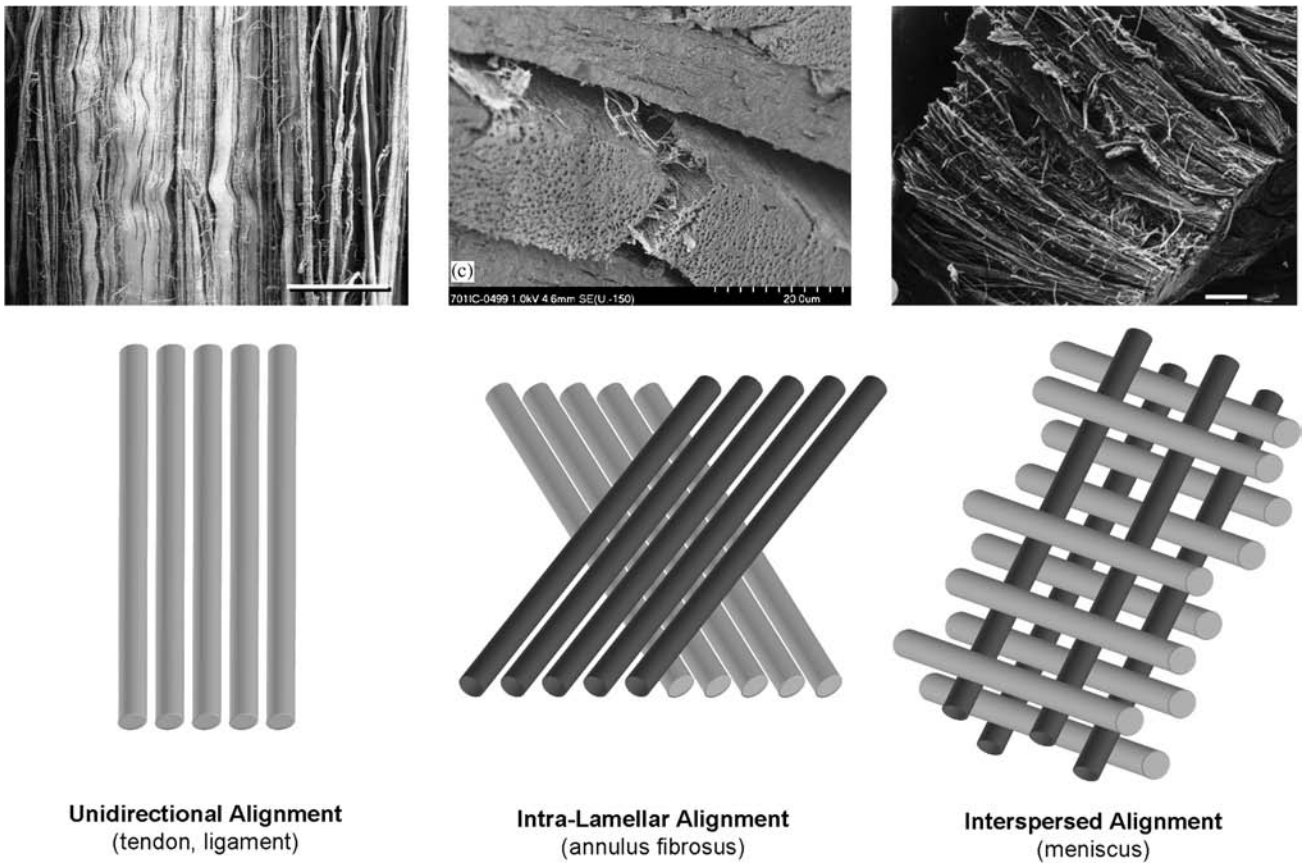

FIG. 1. Fiber organization in dense connective tissues. Most tendons and simple ligaments show fiber alignment in a common prevailing direction over which load is transferred. Annulus fibrosus (AF) and meniscus achieve fiber reinforcement in more complicated loading environments through multilamellar planar alignment of extra-cellular matrix (ECM) or via interspersion of fibers perpendicular to the predominant fiber direction. Image on left from Ref.[137] Scale bar = 100 μm, used with permission from Wiley. Middle image from Ref.[138] Scale bar = 200 μm, used with permission from Elsevier. Right image from Ref.[139] Scale bar = 500 μm, used with permission from Springer.

early in gestation.[5–7] Cell orientation and cytoskeleton polarity is followed by sequential deposition of ECM components (e.g., fibronectin and laminin), which in turn serves as a template for structural protein (collagen) deposition and assembly in an orderly fashion.[5,8] This dense network is then refined and remodeled with load-bearing use to achieve the unique mechanical properties of adult tissues. In addition to these mechanical characteristics, these tissues also share a common feature that in the adult, the matured structures are increasingly hypovascular and hypocellular. Shown, for example, in Figure 2 is H&E staining of fetal compared to adult meniscus, demonstrating the early alignment of formed collagen, and the decreasing cellularity that occurs with age.

While critical for musculoskeletal function, the demanding mechanical environment in which these tissues perform predisposes them to damage. Likewise degenerative changes that occur in all tissues with aging are inadequately counterbalanced by regeneration. As a consequence, tendon and ligament injuries are common; ACL rupture occurs at a rate of 1 in 3000 in the general population of the United States each year (~100,000 ACL tears per year).[9] Similarly, there are more than 750,000 operations performed each year to repair or remove damaged or degenerate meniscus.[10] Failed conservative treatment of lumbar disc herniation leads to surgical discectomy at a rate of over 250,000 per year, making it the most frequently performed neurosurgical procedure in the United States.[11] Notably, the rate of re-herniation is nearly 20%, often occurring at the same disc location.[12] In all of these instances, the limited vascularity and the hypocellularity of these tissues in the adult engender only limited endogenous repair processes. Indeed, this repair does not restore normal tissue structure and function, and the once highly ordered tissue is instead replaced by a disorganized scar, that is, mechanically inferior and prone to re-injury.[7,13,14] Thus, there exists an unmet clinical need for a mechanically functional implantable tissue or tissue substitute that can either guide repair or replace damaged fiber-reinforced tissues.

Approaches to fibrous tissue repair and regeneration

Engineering of functional replacements for these complex fiber-reinforced structures is and remains a daunting challenge to the field. These tissues are dense, avascular, and hypocellular, have refined direction-dependent mechanical properties and hierarchical structures, and function in a demanding mechanical environment. All of these unique characteristics must be considered and enabling technologies must be developed to affect repair for these challenging load-bearing

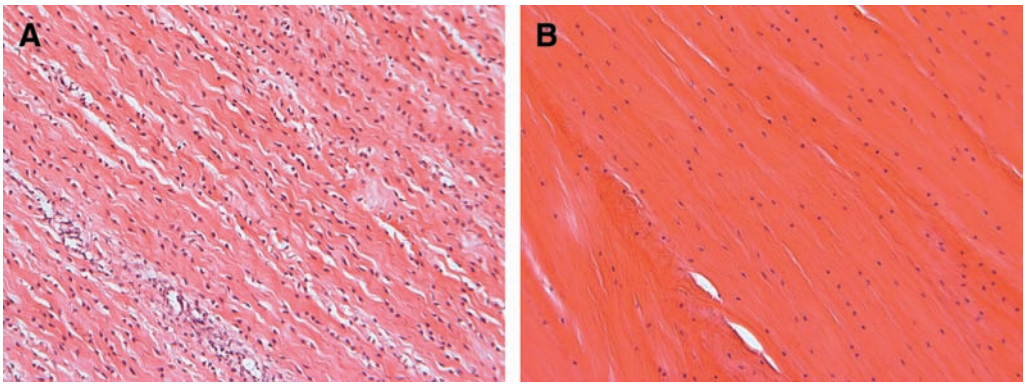

FIG. 2. Cell and matrix characteristics of fiber-reinforced connective tissues. H&E staining of (**A**) fetal ovine meniscus (130 days gestation) and (**B**) adult ovine meniscus (1 year old). With aging, fibrous tissues decrease in cellularity while the collagen-rich ECM grows denser and more organized. Color images available online at www.liebertonline.com/ten.

tissues. To this end, a number of strategies have been developed for tissue repair and replacement. The most sensible and oft tried is the simple replacement of these tissues with similar structures taken from cadaveric donor tissue or alternative donor sites in the patients own body. It has been shown that devitalized (acellular) tendon grafts are re-colonized by fibroblasts from adjacent tissues, and that these cells take on a preferential alignment coincident with the pre-existing collagen network.[15] In practical applications, patellar tendon transfer (in bone-tendon-bone units) is commonly employed in the repair of intra-articular ligaments such as the ACL.[16] Meniscus transplantation from cadaveric sources is also relatively common in clinical practice. With meniscus transplantation, it has been shown that some cellular re-colonization can be achieved over 6 months, though the central core remains devoid of cells.[17] Both techniques are limited, however, by the availability and proper size of donor tissues, the creation of points of donor-site morbidity, concerns related to disease transmission, and the observed decline in tissue properties as remodeling events transpire post-implantation.

To overcome these challenges, numerous tissue engineering strategies have been developed toward the production of fibrous tissues. These constructs can be matured *in vitro* and implanted with fully functional properties, or be designed to mature *in situ* with controlled rehabilitative regimens. Ultimately, the construct needs to operate under loading conditions experienced by the tissue *in vivo*.[18] Toward this end, some of the earliest work in this field was carried out in collagen gels. These studies took advantage of the fact that fibroblast-like cell-mediated contraction around a fixed boundary (a post for example) generates ordered cellular and ECM networks.[19,20] These findings have been extended to more complicated structures with different organization under a variety of boundary constraints.[21,22] While useful for understanding the developmental antecedents of fiber-reinforced tissues, the resulting mechanical properties of most gel-based constructs remain very low, potentially limiting their *in vivo* application. To address mechanics specifically, others have turned to natural and synthetic scaffolds for implantation. These efforts have included woven and nonwoven fibrous scaffolds composed of a diverse range of materials, from standard biodegradable polyesters to silk fibroin.[23] Novel weaving technologies have further refined the mechanical response of such constructs, and commercial products based on these approaches are making their way to market.[24–27]

The approach that we and others have adopted for fiber-reinforced tissue engineering builds on these past efforts, but focuses specifically on the multiscale rendering of fiber reinforcement from the nano- and micron-scale through to the tissue level. These efforts employ electrospinning of ultrafine or nanofibrous polymer networks as a base technology. This review is intended to serve as a general overview of this unique scaffold fabrication technology, and to specifically discuss the mechanical characterization of such scaffolds. In subsequent sections, we discuss the intrinsic properties of natural and synthetic nanofibrous assemblies, methods for instilling anisotropy in these networks, relevant testing modalities as they relate to physiologic loading, and modeling approaches that provide additional insight into scaffold formation and cell-mediated tissue growth. Finally, we provide several case examples where these guiding principles have been deployed toward the engineering of fiber-reinforced tissues, and discuss the challenges that must be overcome for the clinical translation of this technology for the repair of damaged or diseased fibrous tissues.

Electrospinning of Nanofibrous Assemblies

Overview of electrospinning

The technique of electrospinning to create fibrous scaffolds is becoming increasingly prevalent in the extant literature. While the basic technique was first patented in the 1930s,[28] a search for nanofiber or electrospinning in the PubMed database finds nearly 300 entries in the last 12 months alone, with applications as diverse as bone tissue engineering to drug delivery to treatment of burns. Several recent reviews on electrospinning[29–34] highlight much of this literature and provide an excellent foundation for the basic technology and its potential applications. Given the availability of these recent reviews, it is not the intent of this work to review all of electrospinning literature, but rather to focus on those features of electrospun scaffolds that have not been discussed in great detail—namely, the mechanical properties of nanofibrous networks, how these properties are properly assessed and understood, and which considerations must be appreciated for application in load-bearing conditions, and, in particular, the engineering of fibrous tissues.

The basic electrospinning setup consists simply of a polymer source (or sources), a high voltage power supply, and a grounded target (Fig. 3). The solution is expressed through a fine capillary or syringe (called the spinneret) by gravity or positive pressure, and forms a pendant droplet. Application of a high voltage to this solution causes charge buildup and charge–charge repulsion among the individual polymer chains within the droplet, until these intermolecular forces overcome the surface tension holding the droplet in place. Once this critical threshold is reached, the polymer emits from the spinneret as a fine jet, and rapidly travels to the nearest grounded surface.[35,36] As the jet is drawn from its source through the high-voltage gradient, solvent evaporation and whipping instability produces ultrafine fibers (50–1000 nm).[37] With time, these fibers accumulate on the grounded surface to create a mesh composed of randomly oriented fibers. Mesh thickness can be controlled by simply increasing the time of deposition. Nanofiber features in the network depend on the polymer composition and several controllable processing variables[37] (discussed below). Nanofibers can be tuned to range from as small as 50 nm up to several microns in diameter, and as such are many times smaller than most mammalian cells; in fact, they are similar in scale to collagen fibers normally present in the ECM.[38] This nano- and micron-scale topography has been shown to modulate cell signaling pathways[39] and to elicit superior metabolic and matrix forming activities by seeded cells.[40] Nanofibrous meshes are porous structures with a continuous distribution of pore sizes in the range of 2–465 μm and void volumes of 80–90%.[41]

Electrospinning synthetic and natural polymers

Production of meshes via electrospinning has been carried out with numerous polymers, including polyurethanes,[42] biodegradable polyesters (e.g., polycaprolactone [PCL],[41,43–45] polyglycolic acid,[46] polylactic acid,[47–49] and polydiaxanone[50]), and natural biopolymers, including collagen,[44,51–54] elastin,[53,54] silk fibroin,[55,56] chitosan,[57,58] dextran,[59] and wheat gluten.[60] Additionally, liquid blends of biosynthetic and natural components have been electrospun (with components thus mixed in every fiber) to create meshes with enhanced cell compatibility.[61,62] The most common appearance of such blends is in the combination of two dissimilar synthetic materials to result in a blend fiber that has properties of both, or a natural and a synthetic fiber combined to impart biologic functionality to the fibers as they form.[63] Additional studies have modified fiber surfaces to enhance cell binding and/or growth factor retention.[64–66] Further, methacrylate-based copolymers have been electrospun to form nanofibrous coatings that can be crosslinked after formation.[67,68] We have recently reported on the electrospinning of several elements of a library of 120 poly(β-aminoester)s that were photo polymerized after formation[69] as well as novel photocrosslinkable and hydrolytically degradable elastomers.[70] Clearly, there exists a wide range of polymers that can be processed into the nanofibrous format.

Optimization of electrospinning parameters

For each polymer utilized, spinning parameters are optimized to generate a homogeneous fiber array. Common intrinsic parameters that can be varied include the solvent type and composition, the mass concentration of the polymer, molecular weight of the polymer, solution viscosity, applied voltage, electric field strength, spinneret-to-collector distance, and polymer flow rate.[30,36,37,71] Additional extrinsic parameters include atmospheric conditions such as ambient temperature and humidity. These individual parameters are

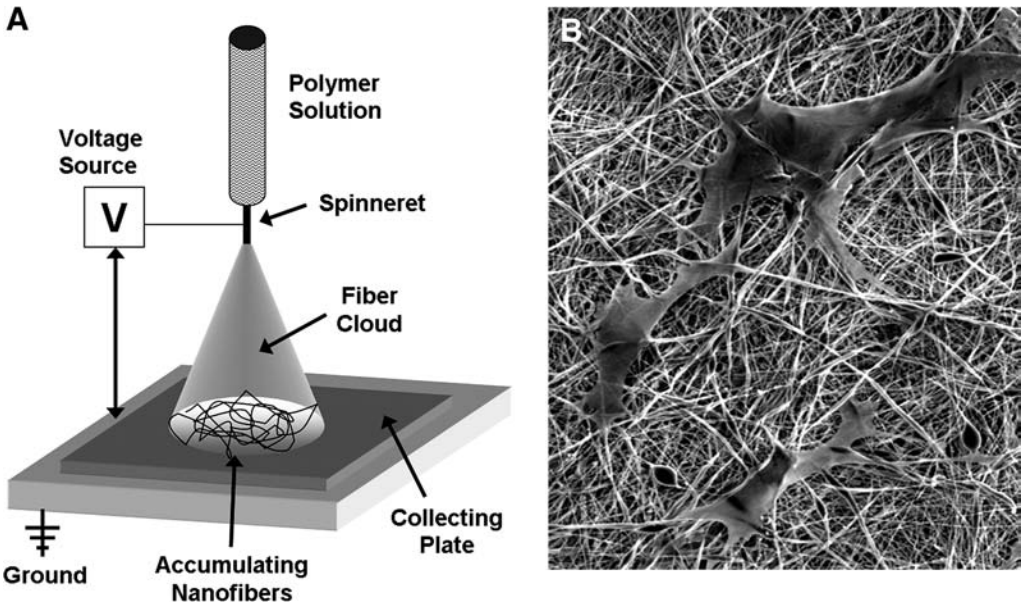

FIG. 3. Electrospinning ultrafine fibrous networks. (**A**) Schematic of a common electrospinning setup. These simple systems consist of a polymer source flowing (actively or passively) through a highly charged spinneret, where charge repulsion in the solution generates a dispersion of fiber jets that travel rapidly to a grounded collecting plate or mandrel. (**B**) Electrospun fibers have diameters that range from 50 nm to several microns, providing a surface topography in which cells interact simultaneously with multiple fibers. Shown are human mesenchymal stem cells (MSCs) on a nonaligned polycaprolactone (PCL) nanofibrous sheet.

tuned to generate fibers that meet the criteria of the intended application, most commonly that the fibers minimize their diameter, be free of defects (beads), and show little fiber–fiber welding at the interstices. Figure 4A shows examples of such defects in a PCL scaffold formed with suboptimal electrospinning conditions. Fiber diameter and defects can usually be controlled by adjusting the solution mass concentration, voltage gradient, and distance over which fibers are collected. Solvent characteristics strongly influence these features. A recent study by Kidoaki and co-workers showed that when electrospinning poly(ester urethane)urea (PEUU), increasing *N*,*N*-dimethylformamide content in the spinning solution led to enhanced fiber–fiber welding.[72] In some cases, for example, when the molecular weight is low, polymers simply cannot be electrospun on their own using traditional measures. In such instances, alternative strategies must be adopted. In our recent efforts to electrospin low-molecular-weight photocrosslinkable macromers from a poly(β-aminoester) library, a carrier molecule, poly ethylene oxide (PEO), was required to increase the viscosity and chain length of the polymer solution.[69] Once formed, nanofibers of this kind could be stabilized by photocrosslinking, and the carrier removed. In other applications, synthetic polymers that are readily spun on their own have been used as carriers for biologic proteins, such as collagen and elastin, which are generally more difficult to spin and/or stabilize after production.[62,63,73]

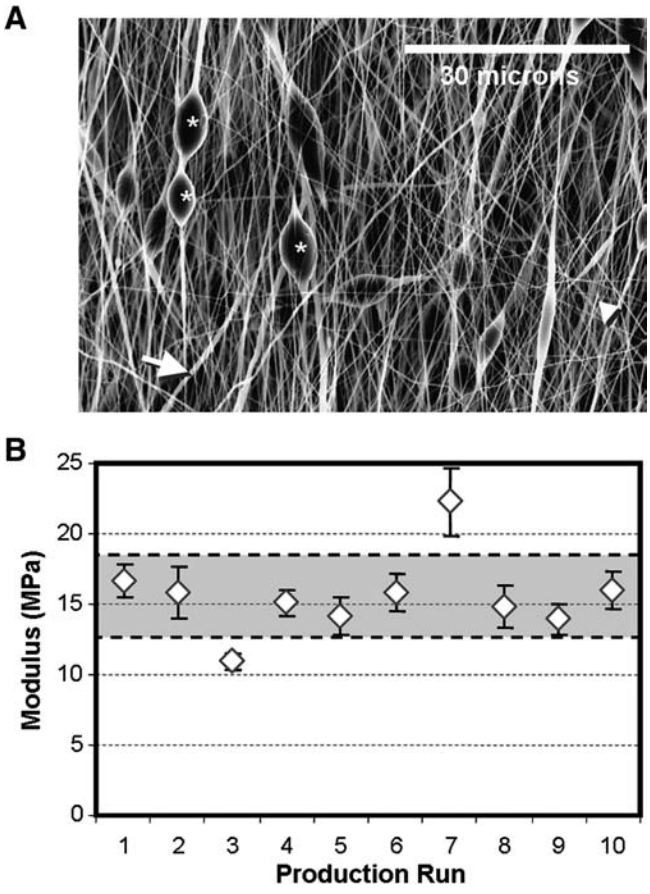

FIG. 4. Optimization of electrospun scaffolds. Solution, fabrication, and environmental parameters can be optimized to generate sheets with homogenous fiber populations. Shown in (**A**) are several features that arise when electrospinning conditions are not optimized; *, bead-like inclusions; large arrow, thick fibers; small arrowhead, thin fibers. Quality control of microstructure is required to ensure homogeneity across production runs. Even when precautions are taken, small changes in fiber properties can yield a range of mechanical properties in the resultant scaffolds. Shown in (**B**) is the modulus of aligned PCL scaffolds produced over 10 separate production runs. Note the deviations in mechanical properties within each batch, as well as the scatter of average properties across production runs. Gray area indicates ±1 standard deviation for this grouping of scaffolds.

Even after spinning conditions have been optimized, some variation exists between batches, most likely caused by small changes in extrinsic and intrinsic conditions on the day of production. Indeed, some in the field have suggested that electrospinning is an art rather than a science because of this inherent variability. An example of this is shown in Figure 4B, where the mechanical properties of 10 different batches of PCL nanofibers (aligned, tested in the fiber direction) show some intra-scaffold variability (based mostly on position on mandrel), and extensive intra-batch variability (from small deviations in intrinsic and extrinsic factors). In our studies, we address these concerns in two ways. First, when multiple scaffolds produced on different days are to be combined for use in a large study, rigorous characterization (structural and mechanical) is carried out on each batch, and those not matching desired criteria are removed. Second, when using scaffolds for a cell-based study, we commonly include acellular controls to be tested in the same manner and at the same time points for the duration of the study. These steps have increased consistency between studies, and have aided in the interpretation of research findings.

Order from Disorder: Methods for Inducing Anisotropy

When standard electrospinning methods are employed, and fibers are collected onto a stationary grounded plate, the resultant mesh contains fibers organized in a random fashion. As indicated above, most fiber-reinforced tissues show pronounced mechanical anisotropy (different properties in different directions), which is based on the underlying organized collagen ultrastructure. Methods to induce fiber alignment in nanofibrous scaffolds have thus been of great interest to the fiber-reinforced tissue engineering community, and were recently reviewed by Teo and Ramakrishna.[31] One of the first instances of nanofiber alignment was presented by Theron and colleagues,[74] who focused fiber collection on the thin edge of a rotating disk. Nanofiber alignment was also demonstrated by Xia and colleagues, using a system in which the collecting surface was composed of pairs of electrodes that could be differentially grounded and separated by an air gap or insulating surface. In this way, linear arrays of fibers were generated, and by varying the state of the electrodes (grounded or not), different rosette patterns were achieved.[32,75,76] More recently, Sun and colleagues[77] demonstrated the capabilities of near-field electrospinning, where a point spinneret is situated only a few microns from the grounded surface. The probe tip, which is dipped in polymer solution, becomes a stylus from which polymer is ejected, and its position relative to the ground can be controlled to fabricate ordered structures. These methods are somewhat limited in their throughput; therefore, the most common

method for aligning fibers for the generation of tissue engineering scaffolds (and the method that our lab uses) is to deposit fibers onto a rotating drum or mandrel.[78–84] From high-speed imaging studies, it has been shown that a single fiber can transit from the source spinneret to the ground at speeds >2 m/s.[85] Thus, presenting a surface moving faster than the fiber jet will pull fibers into alignment as they are deposited. We and others have shown that the degree of alignment is a function of the rotation speed of the collecting surface.[81,83,84] Further, this structural anisotropy is reflected in the measured mechanical properties, with more highly aligned scaffolds possessing greater levels of mechanical anisotropy.[81]

Mechanical Characterization of Nanofibrous Scaffolds

Mechanical properties of nanofibrous assemblies

Most load-bearing tissue engineering applications with nanofibrous scaffolds require some level of mechanical functionality. Therefore, the most common assay (aside from scanning electron microscopy observation) of any nanofibrous scaffold is the assessment of mechanical properties. These properties are typically assessed at the time of formation, as well as with subsequent degradation under physiologic conditions or with cell-mediated matrix deposition. When formed into random or nonaligned meshes, nanofiber scaffolds exhibit isotropic properties (same in all directions) that are reflective of the mechanical properties of their polymer composition. For example, polymers such as poly(D,L-lactide-co-glycolide) (PLGA) produce meshes that are quite stiff in tension, while scaffolds composed of PCL are 10 times less stiff and remain elastic over a wider range (up to 8–10%)[49] (Fig. 5). When biologic and synthetic molecules are mixed (in the same solution) before electrospinning, mechanical properties vary with composition.[34,73] Given the large number of polymers (as well as biopolymers) that have been successfully electrospun, there is a correspondingly wide range of mechanical properties that can be achieved (see Table 1). Multi-jet electrospinning systems have also been developed to increase production rates.[29,86–88] These systems may be used to create composite scaffolds (with a different polymer in each jet) whose properties reflect the properties and ratios of the individual components.[89–94] Several such multicomponent scaffolds are described in detail below.

In addition to properties imparted by the polymer composition itself, several other factors may influence the measured mechanical properties. As noted above, recent studies have shown that alignment and mechanical properties in the fiber direction increase substantially as the collecting surface (rotating mandrel) increases in velocity.[81,83,84] For example, for PCL scaffolds, the ratio of properties in the fiber direction compared to transverse to the fiber direction can increase by 10–20-fold with increasing alignment[81] (Fig. 6). Testing aligned scaffolds in directions that do not correspond to the prevailing fiber orientation also influences the measured mechanical properties in a predictable fashion.[82] Random scaffolds exhibit a relatively linear stress–strain response in the pre-yield region, and extend linearly after yield. Aligned scaffold tested in the fiber direction have a sharper increase in stress with increasing deformation, and yield and fail at similar points earlier in the strain regime. When these same scaffolds are tested in the transverse direction, a much lower stress–strain profile is observed. Other factors that can change mechanical

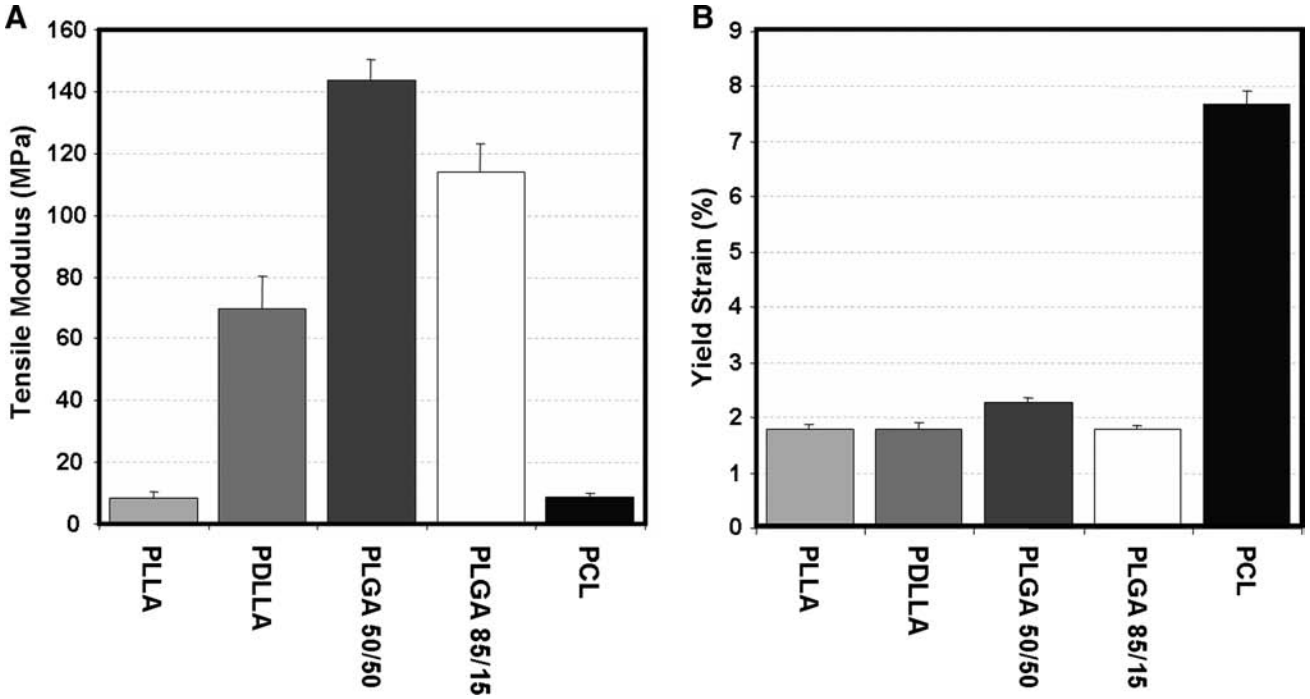

FIG. 5. Tensile properties of common biodegradable polymers. (**A**) Tensile modulus and (**B**) yield strain for nonaligned nanofibrous scaffolds fabricated from a common set of biodegradable polymers. A range of properties can be achieved, but few polymers can be distended to greater than 2% elongation before yielding. Adapted from Ref.[49] with permission from Elsevier.

Table 1. Tensile Properties of Common Electrospun Scaffolds

	Polymer	Alignment	Modulus (MPa)	Yield strain (%)	Ultimate strain (%)	Yield stress (MPa)	Ultimate stress (MPa)	References
1	Thermoplastic polyurethane	Both	n/a	n/a	n/a	n/a	n/a	139
2	Polydiaxanone-elastin blend	NA	5–10	n/a	60–200	n/a	3–5	63
3	Poly(ester urethane)urea	NA	8	n/a	2.2	n/a	13	140
	Poly(ester-urethane)urea-collagen blends	NA	1–7	n/a	160–280	n/a	2–11	140
4	Biodegradable polyurethane	NA	5.7	61	79	61	1.3	141
5	Poly(D,L-lactide-co-glycolide) (85:15)	NA	323	n/a	96	n/a	23	41
6	Poly(p-diaxanone-co-L-lactide)-block-poly(ethylene glycol)	NA	n/a	n/a	n/a	n/a	1.3–1.4	142
7	Silk fibroin	NA	625	n/a	4	n/a	13.6	143
8	Poly(L-lactide-co-ε-caprolactone)	NA	156	n/a	127	n/a	5	43
9	Collagen-poly(ethylene oxide) blends	NA	12	n/a	n/a	n/a	0.37	144
10	Collagen	AL	52.3 26.1	n/a	n/a	n/a	1.5 0.7	51
11	Poly(ethylene glycol)-g-chitosan	NA	n/a	n/a	78–112	n/a	8–17	145
12	Gelatin	NA	105	n/a	64	n/a	2.5	73
	Gelatin-poly(ε-caprolactone)	NA	5	n/a	126	n/a	2.7	73
	Poly(ε-caprolactone)	NA	31	n/a	138	n/a	1.3	73
13	Poly(vinyl alcohol)-cellulose acetate blends	NA	44	n/a	420	10	11	88
	Poly(vinyl alcohol)	NA	18–34	n/a	214–334	5.9–7.2	7.0–9.4	88
	Cellulose acetate	NA	3	n/a	175	1.5	2	88
14	Poly(L-lactic acid)	NA	8.5	1.9	20–25	0.1	n/a	49
	Poly(D,L-lactic acid)	NA	70	1.9	n/a	1.1	n/a	49
	Poly(D,L-lactic-co-glycolic acid) (50:50)	NA	144	2.1	38	2.8	n/a	49
	Poly(D,L-lactic-co-glycolic acid) (85:15)	NA	114	1.9	n/a	1.9	n/a	49
	Poly(glycolic acid)	NA	138	2.1	n/a	2.7	n/a	49
	Poly(ε-caprolactone)	NA	8.5	7.5	n/a	0.7	n/a	49
15	Poly(ε-caprolactone)	AL	3.3–4.7 2.7–3.9	n/a	200–231 216–277	0.6–0.7 0.6–0.4	1.4–2.1 1.2–2.0	146
16	Poly(glycolic acid)	AL	55–105 20–55	n/a	60–80 105–130	n/a	n/a	78
	Poly(glycolic acid)	NA	40–95	n/a	80–100	n/a	n/a	78

Mechanical properties of electrospun scaffolds for fibrous tissue engineering. Depending on the choice of polymer and formation method, electrospun scaffolds can achieve a range of mechanical properties. For example, the modulus can range from one to several hundred MPa. Moreover, yield strains can be quite low for many common biodegradable polyesters, but markedly higher for elastomeric polymers.

NA, nonaligned; AL, aligned; n/a, not available.

properties include the amount of solvent remaining in a fiber when it reaches the collecting plate and consequently the number of fiber–fiber welds that form. Kidoaki and co-workers showed a fourfold increase in properties of electrospun scaffolds with increasing degrees of fiber–fiber welding.[72] Some materials show profound changes in mechanical properties when they are tested in a dry versus hydrated state. For example, collagen nanofibers (which must be cross-linked to be hydrated) decrease in tensile properties by approximately 100-fold with hydration.[95,96] In composite fibers formed with a temporary carrier (such as PEO), bulk scaffold properties may change as the carrier material is eluted. We have shown, for example, that mechanical properties can increase in scaffolds that are cross-linked after formation, and then subsequently decrease as the carrier PEO is eluted.[69] Given the large number of factors influencing these mechanical properties, and the importance of these properties for fiber-reinforced tissue engineering applications, the following sections describe nanofiber and scaffold evaluation across multiple length scales and in different testing configurations.

Single-fiber mechanics

At their most basic level, nanofibrous scaffolds are the sum of many thousands of ultrafine fibers traversing a small volume. While these fibers sometimes interact, via welding or frictional interactions, bulk scaffold properties should build directly from these constituent fibers. Testing of a single fiber is an exacting science, requiring specialized and sensitive equipment, and as such there are few examples in the literature. Of these few, perhaps most common is the microtensile testing of single fibers. In one study by Tan and colleagues,[97] single PCL fibers were collected across a small gap, and uniaxial extension applied until failure was achieved. They reported that smaller fibers have a higher modulus, but are less ductile than larger fibers. Similarly, Chew and co-workers found that small fibers were stiffer than thick fibers, and that individual fiber properties change when model proteins and pharmacologics were incorporated.[98] Subsequent work by Lim and colleagues showed that crystallinity within a fiber strand influenced mechanical behavior; more crystalline fibers

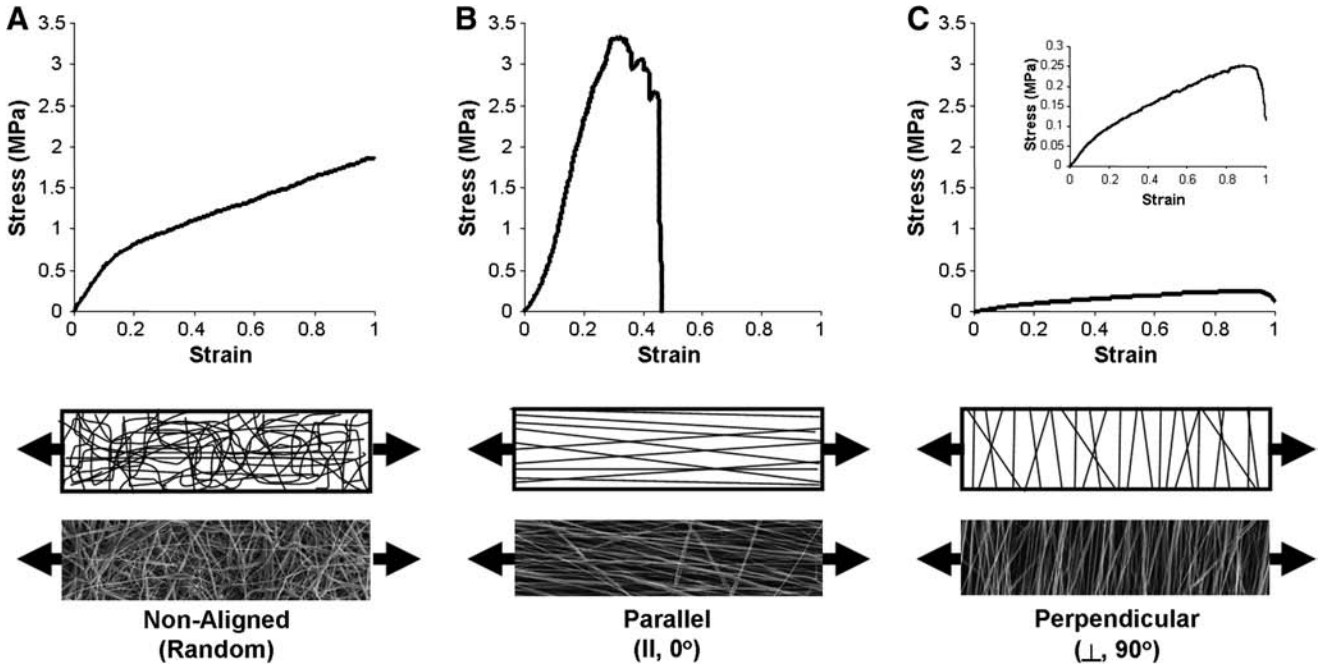

FIG. 6. Fiber alignment influences mechanical properties of nanofibrous scaffolds. Stress–strain response of PCL nanofibrous scaffolds produced in a nonaligned configuration (**A**), produced in an aligned configuration and tested in the prevailing fiber direction (**B**), and produced in an aligned configuration and tested in the transverse direction (**C**). Schematics and images illustrate fiber organization and testing direction for each scaffold.

(produced from lower concentration solutions) were stiffer than less crystalline fibers (even when fiber diameters were comparable).[99] In addition to direct tensile tests, atomic force microscopy (AFM) has been used to manipulate and test single fibers as well. For example, Kim and colleagues showed that cross-linked poly-HEMA nanofibers snap back into place after being distended with an AFM probe tip.[68] Tan and coworkers fixed one end of a nanofiber, and used the AFM cantilever to deform and measure force generated in PEO nanofibers.[100] Similarly, the AFM probe tip has been used to carry out three-point bending tests of individual fibers placed over a groove microetched into a silicon wafer.[101] Still more recently, specialized MEM devices have been constructed that couple with AFM cantilevers, and have been used to show the dependence of ultimate strain on applied strain rate for polyacrylonitrile nanofibers.[102,103]

Uniaxial tensile testing of fibrous assemblies

While scaffolds are comprised of individual fibers with their own set of distinct mechanical features, the mechanical function is most commonly characterized in bulk samples, where the individual fibers combine to produce an aggregate response. In uniaxial testing of bulk scaffolds, load is applied along a single specified direction, while the sample is free to contract laterally. A rectangular or dumbbell-shaped sample is typically loaded into a test frame and pulled at a specified rate of displacement (displacement controlled) or force (load controlled), and both the load and displacement are measured. By normalizing force to undeformed cross-sectional area (engineering stress) and displacement to undeformed length (engineering strain), we can calculate the stress–strain behavior. To evaluate cross-sectional area, noncontacting methods such as imaging or laser systems are preferable; this avoids permanent deformation of scaffolds, particularly at early culture periods. The typical metric for the elastic behavior of linear elastic materials (those in which the plot of stress vs. strain reveals a linear relationship) is the Young's modulus (E), or slope of the stress–strain curve. Some electrospun polymers, such as aligned PCL fibers (as well as many fiber-reinforced soft tissues), exhibit a nonlinear stress–strain behavior and so are characterized by reporting a slope of the beginning of the curve, known as the toe-region modulus, in addition to the elastic region modulus. The strain at which the curve transitions from toe to linear regions is the transition strain, and is an additional parameter of interest in nonlinear materials. When electrospun scaffolds are stretched beyond their elastic regime, they may experience either of two primary failure modes: plastic deformation (deformations that are not reversed upon removal of load) and catastrophic failure (load goes instantly to zero or decreases markedly). The onset of plastic deformation occurs at a strain–stress level known as the yield point. As noted above, electrospun polymers have distinct failure properties, and may involve a combination of yielding and catastrophic failure.[81,104] In this case, an additional material property, the ultimate tensile strength, or the maximum stress before failure, is often reported. However, post-yield measures, such as ultimate tensile strength, are less valuable for tissue engineering than properties of the elastic behavior, because postyield deformations are not recoverable upon unloading. Due to the dynamic loading that most tissues encounter, it is critical that an engineered construct recover after deformation, and not be fully expended after a single loading event. Further, native soft tissues often undergo more than 25% deformation before yielding or failure, while many common polymers in

electrospinning are limited to 1–2% strain before yielding (see Table 1).[49] Therefore, the yield point is an important design criterion to consider when selecting polymers for specific tissue applications.

Biaxial tensile testing of fibrous assemblies

Despite the value and practicality of uniaxial tensile testing, its physiologic relevance is limited because of the absence of freely contracting boundaries for many tissues *in situ*. A great many fiber-reinforced soft tissues, such as the meniscus, AF, arteries, and myocardium, are subject to tensile loads along multiple directions. For this reason, biaxial tensile testing is a more valuable testing modality for electrospun scaffolds and tissue-engineered constructs. Although uniaxial tests can be performed in multiple orientations with respect to the prevailing fiber direction,[51,81,82] these tests must be performed either on multiple samples or sequentially on the same sample at small, sub-yield strains. However, biaxial testing allows for the measurement of the material behavior simultaneously along two orthogonal axes. This method is more robust for characterizing scaffold and tissue function, and more closely approximates *in vivo* loading. Nonetheless, there are relatively few studies that have considered the biaxial behavior of electrospun scaffolds.[83,105–107]

Grip-to-grip versus local strain

In both uniaxial and biaxial tensile testing, it is common to use grip displacement to compute strain.[81,82,95,108] However, as this method only generates information regarding the boundaries of the sample, it introduces errors associated with inhomogeneous strain fields and sample slippage at the grips. Therefore, measurement of material or local strains from the sample mid-substance more accurately reflects the true strain of the material.[109] This is typically performed by placing fiducial markers on the sample, or speckle coating the surface with paint or other texture, and collecting images of the sample surface throughout the test. These images are then postprocessed to measure the surface strains during the deformation. This results in two-dimensional material strains, which, in the case of uniaxial tests, allow for the determination of an important additional material property, the Poisson's ratio. An example of the local strain associated with tensile deformation of an aligned nanofibrous scaffold is shown in Figure 7. Average strain within a region of interest (ROI) compares favorably with the bulk grip-to-grip strain, while clear heterogeneity across the ROI is observed. It is possible, however, that with tissue deposition by resident cells, engineered constructs may produce complex, heterogeneous strain fields and become increasingly susceptible to slippage at the grips. Therefore, it is of value to perform the necessary validations for studies where grip-to-grip strains are employed. On a fiber level, even this characterization of surface strain likely misses fiber rearrangements and sliding more consequential to the response of isolated cells within the network. For example, recent work by Stella and co-workers showed that nuclear orientation and deformation correlated with bulk scaffold deformation up to ~50% strain, and then remained constant thereafter.[107] Methods such as these, where fiber and cells are monitored continuously with applied deformation, will be required to determine the precise local deformations that control cell activity within these scaffolds.

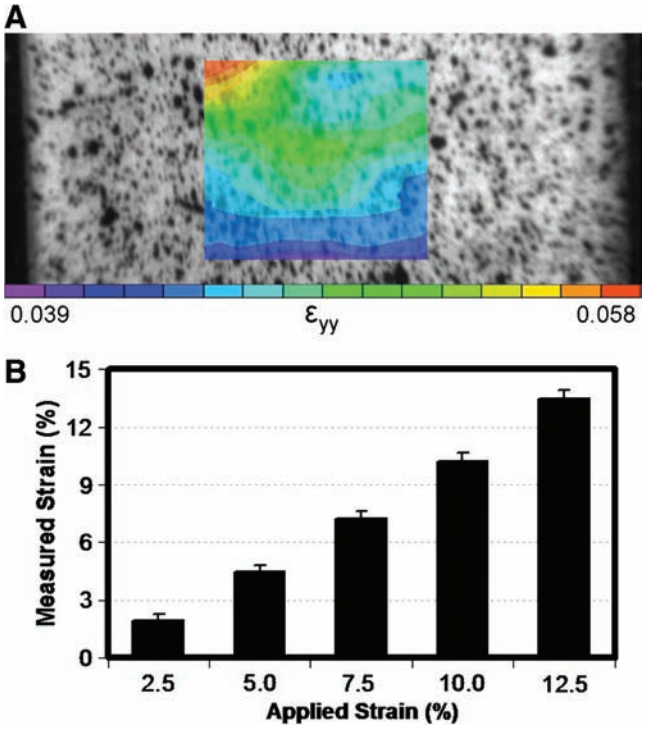

FIG. 7. Local strain in aligned scaffolds with tensile deformation. (**A**) Surface image of speckle-coated scaffolds with superimposed strain map of an aligned nanofibrous scaffold undergoing tensile deformation. Equilibrium strain ranged from 4% to 6% with a grip-to-grip strain of 5% within the ROI. (**B**) Average local strain in ROI compared to grip-to-grip strain for a range of deformations. These data illustrate that bulk deformations of aligned scaffolds are relatively uniform in the center of scaffolds. Color images available online at www.liebertonline.com/ten.

Dynamic and viscoelastic properties of electrospun scaffolds

Although electrospun scaffolds are primarily elastic structures, they are commonly applied to the engineering of viscoelastic and cyclically loaded tissues. Despite this fact, the testing procedure for electrospun scaffolds is typically a quasistatic (slowly applied strain rate to eliminate rate dependent effects), continuous ramp to failure. Based on some theoretical models[81,82] there is evidence that electrospun PCL fibers may slide relative to one another. These frictional interactions may be a source of rate-dependent effects. Moreover, as resident cells deposit ECM on electrospun scaffolds, there is an increase in water content and concentration of viscoelastic ECM elements. In effect, the rate-dependent behavior of electrospun scaffolds and engineered tissues is of great importance; however, this aspect of electrospinning for tissue engineering has not been widely characterized. Further, it is important to understand how electrospun materials behave under conditions of repeated loading. Humans take an estimated 1–2 million steps per year, so materials for implantation must be able to withstand cyclic loading without experiencing fatigue damage. We have recently tested aligned

PCL scaffolds for up to 20,000 cycles of dynamic tensile deformation to 3% grip-to-grip strain at a frequency of 0.5 Hz. Results of this study are shown in Figure 8. Interestingly, the scaffolds showed very little energy loss when dynamically loaded in this strain regime, as evidenced by the small area of hysteresis. Further, there was no apparent change in the tensile modulus or maximum stress of these scaffolds as a consequence of the loading regimen. Conversely, Klouda *et al.* carried out a similar study investigating the effect of cyclic tensile loading on nonaligned electrospun PCL scaffolds for a longer duration. They found a reduction in the failure strain and ultimate tensile stress in samples that were cyclically loaded for 15 days, but no change in the elastic modulus.[110] Additional work by Sell and co-workers employed dynamic compliance testing to evaluate polydiaxanone-elastin nanofiber tubes for vascular applications.[63] These results suggest that experiments such as these, assessing dynamic and fatigue properties, are particularly relevant for tissue engineering strategies that may exploit cyclic loading bioreactors or involve direct implantation into load-bearing sites.

Modeling of Nanofibrous Scaffold Mechanics

Although experimental measures of mechanical function are instructive, theoretical or constitutive models provide additional insight into the study of both acellular scaffolds and the maturation of cell seeded constructs. A constitutive model is an explicit mathematical description of the mechanical behavior of a material. Constitutive laws permit the mechanical characterization of complex materials and, more importantly, permit one to predict how a material will behave in response to various mechanical perturbations. Despite their utility, constitutive models have not been widely used to describe electrospun scaffolds, and have been used even less to describe nanofiber-based engineered tissue constructs.

Constitutive models of electrospun scaffolds vary widely in their complexity, from simple geometrically motivated linear models[81,82,108] to hyperelastic continuum models.[83,111,112] Mathew *et al.* successfully predicted the dependence of electrospun poly(butylene terephthalate) mechanics in uniaxial tension on the degree of alignment and prevailing fiber orientation using a classical equation from fiber-reinforced rubbers.[108] In a similar application, Li *et al.* used a linear spring model that accounted for fiber dispersion to predict the response of electrospun PCL scaffolds; the model closely approximated the experimentally measured dependence of modulus on degree of dispersion only when it permitted unconstrained sliding between fibers.[81] Nerurkar *et al.*[82] applied a linear homogenization model to characterize the dependence of aligned PCL on fiber orientation in uniaxial tension, demonstrating that fiber connectivity and nonfibrillar matrix are key determinants of this relationship. This work

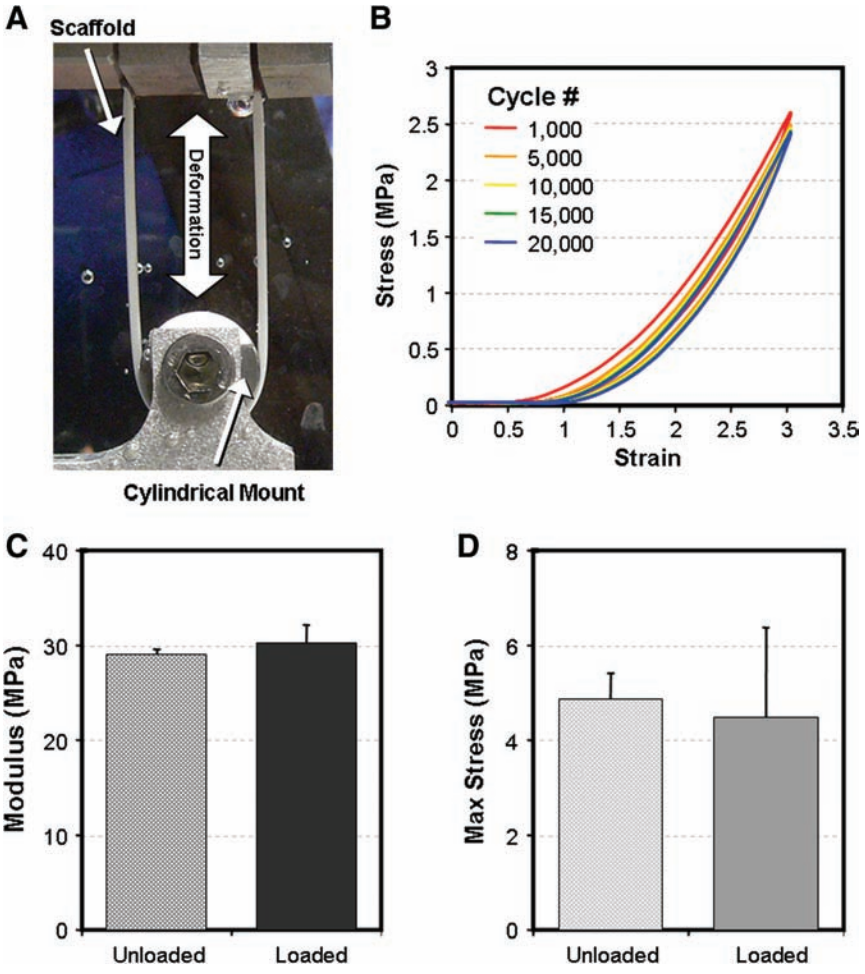

FIG. 8. Dynamic testing of nanofibrous scaffolds. (**A**) Setup for dynamic and fatigue testing. (**B**) Dynamic stress–strain profiles of aligned nanofibrous scaffolds through 20,000 cycles of 3% deformation applied at 0.5 Hz. (**C**) Modulus and (**D**) maximum stress of constructs before and after 20,000 loading cycles. Color images available online at www.liebertonline.com/ten.

also confirmed the observation by Mathew *et al.* that fiber orientation plays a minimal role in the uniaxial tensile behavior of aligned electrospun fiber mats when the direction of loading deviates by more than 40° from the prevailing fiber direction.

Hyperelastic models have the additional advantage of describing materials with nonlinear mechanical behaviors over large deformations. Because nonlinearity and finite deformations are functional signatures of many fiber-reinforced soft tissues, hyperelastic models are of great value not only for characterizing acellular scaffolds and engineered constructs, but also to yield comparisons of these materials with native tissue benchmarks. De Vita *et al.*[111] employed a hyperelastic model to describe the elastic and failure behavior of aligned electrospun poly(butylene terephthalate), whereby failure was modeled as a statistical distribution of fiber failure strains at which fibers ceased to carry load. Although the model was able to fit both elastic and postyield behavior with relative accuracy, interpretation of these types of models is limited by an inability to distinguish between the catastrophic and sequential failure of fibers and the plastic deformations that are likely superimposed upon them. Courtney *et al.*[83] formulated a hyperelastic model that incorporated fiber distributions, and applied it to ES-PEUU scaffolds with varied degrees of alignment. One key feature that distinguishes this study from those discussed thus far is the application of the model to biaxial tensile tests. Unlike Nerurkar and colleagues and Mathew and co-workers, who investigated multidirectional properties by uniaxial tension, modeling biaxial tension is a more robust method because the model must simultaneously describe behavior along two orthogonal loading directions.

By fully characterizing the mechanics of an acellular scaffold, constitutive models can also be used to characterize changes in mechanics subsequent to the deposition of ECM by a resident cell population. In effect, constitutive models can serve as quantitative measures of functional maturation for cell-seeded constructs. This was proposed in Nerurkar *et al.*[82] for a linear homogenization model, and later extended to a nonlinear hyperelastic model by Nerurkar *et al.*[112] (described below). In this study, the authors used the material parameters of a fiber-reinforced constitutive model as metrics for functional growth of engineered AF constructs, and correlated these metrics with biochemical composition. Additionally, upon validation, the model was used to investigate (by simulation) the consequences of construct maturation on complex, physiologically motivated loading scenarios such as biaxial tension and simple shear. At their basic level, models of these systems may provide insight into the complex molecular interactions of native tissue, and be used to guide model development for these more complicated assemblies. For tissue engineering, modeling of complex dynamic scaffolds of varying composition can be used to tune construct properties to match the necessary mechanical requirements expected over the lifetime of its intended use.

Fibrous Tissue Engineering on the Straight and Narrow

Many polymers, many choices

Given the large and growing number of polymers available for electrospinning, their unique mechanical and degradation characteristics, and the ability to precisely control their organization, the question arises: How does one choose a starting point for tissue engineering applications? The answer to this question must be in part defined by the cell population and matrix organization of the tissue of interest as well as the operating conditions experienced by that tissue. Cellular interaction is of course important, both in the case of acellular scaffolds to be colonized after implantation, as well as cellularized constructs grown *in vitro*. While fibrous tissues are unified in their hierarchical matrix organization, some are more organized than others (compare for example the supraspinatus tendon with the flexor tendon), and scaffolds should reflect this complexity. The approach to tissue replacement matters as well; a construct intended for immediate implantation will require different properties than one that is matured *in vitro* before implantation. For example, if the tissue of interest is one that commonly experiences *in vivo* strain levels of >5% strain, then polymers that yield below this level may be unsuitable for immediate implantation. However, these same polymers, combined with the appropriate cell source *in vitro*, may be perfectly acceptable if the cell-mediated deposition of new ECM allows for a greater range of distensibility after some culture duration. Alternatively, controlled rehabilitation regimes after surgery might be employed to protect the implant from loading while *in vivo* maturation takes place. At the end of the production and/or maturation process, the implanted material on functional day 0 should duplicate as many of the natural features of the native tissue as possible. For example, while the linear modulus of tendons and ligaments is important, the toe region is just as important, if not more so. As measured by Butler and colleagues, the normal operating range of a tendon does not typically engage its failure state.[113] Indeed the toe region is critical for ensuring low-force mobility of joints and other moving structures to enable smooth motion, while the failure properties are operative only under extreme conditions.

Case example: knee meniscus

One tissue for which we have extensively investigated the application of nanofibrous scaffolds is the knee meniscus. As noted above, this fibrous tissue of the knee functions to transmit load from the femur to the tibia, and enhances joint congruency. A distinguishing feature of the meniscus is the highly organized collagen fiber structure, which imparts to the tissue anisotropic tensile properties. An example of the stress–strain response of meniscus (tested in the fiber direction) is shown in Figure 9. From this plot, we can appreciate that the tissue shows significant nonlinearity in its stress–strain response, with clear toe and linear regions. Also shown on this plot are the stress–strain profiles of several aligned nanofibrous constructs of differing polymer compositions (all tested in the aligned fiber direction). As can be readily observed, some of these polymers result in scaffolds that are stiffer than the native tissue and fail at much lower strain levels, while others produce scaffolds that are considerably less stiff, matching at best the toe region modulus of the native tissue.

Of the many possible polymers, we work primarily with PCL, a slow degrading polyester that matches the native tissue in its toe region, shows some nonlinearity in its stress–strain response, and is distensible to greater than 10% strain. In most of our studies PCL is formed into nanofibers using the

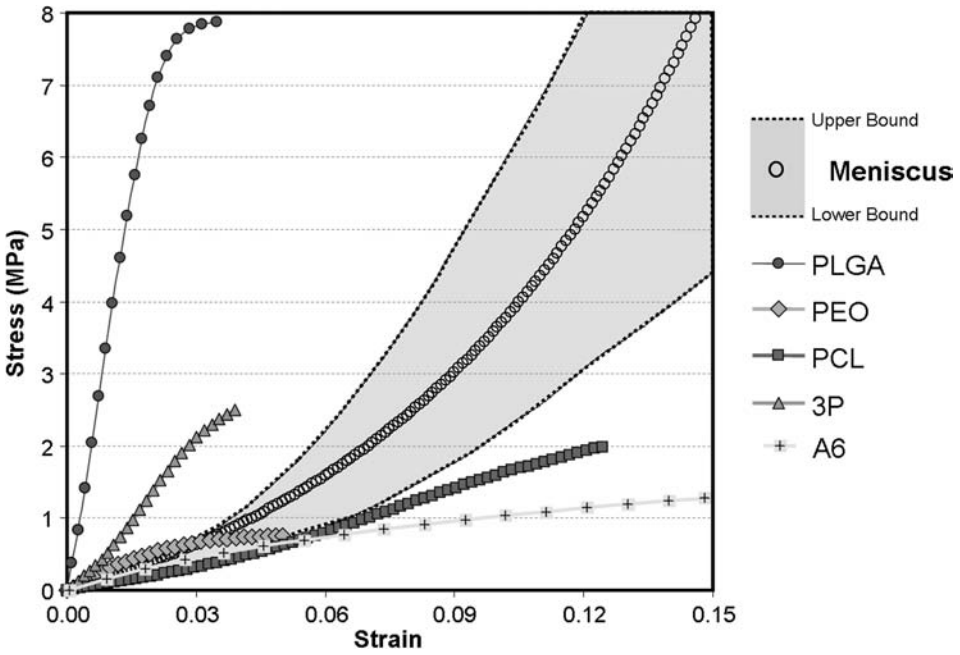

FIG. 9. Benchmarks for the engineering of fibrous tissues. Healthy meniscus tissue tested in the fiber direction produces a nonlinear stress–strain response (circles indicate average response; boundaries indicate high and low range of responses from 10 separate samples). Superimposed on this physiologic range are the stress–strain responses of nanofibrous scaffolds of varying composition.

electrospinning process, and scaffold fiber organization is tuned by collecting on a static surface (for nonaligned scaffolds) or on a rotating mandrel (when alignment is desired).[80–82] In one recent study, we evaluated the long-term *in vitro* maturation of scaffolds after seeding with either mesenchymal stem cells (MSCs) or meniscus fibrochondrocytes (MFCs). MSCs are multipotent cells derived from bone marrow that can undergo fibro-cartilaginous differentiation, while MFCs are cells derived from the native tissue that are normally responsible for the production and maintenance of the fibro-cartilaginous ECM. Cell infiltration and construct maturation were evaluated as a function of topography with culture on both aligned (AL) and nonaligned (NA) scaffolds.[80] Seeded scaffolds were cultured in a defined prochondrogenic medium[114] for 10 weeks and at bi-weekly intervals, and were tensile tested to failure; their biochemical and histological characteristics were assessed.

The results of this study showed that aligned nanofibrous scaffolds direct cell polarity in the scaffold (Fig. 10). At the outset of the study, AL scaffolds had a higher linear region tensile modulus ($\sim$12 MPa) than NA scaffolds ($\sim$4 MPa). Notably, PCL degrades slowly, and so mechanical properties did not change over 70 days in the absence of cells (not shown). When seeded with MSCs or MFCs, both AL and NA scaffolds increased in tensile properties with time (Fig. 11). AL constructs increased by $\sim$10 MPa, while NA constructs increased by only $\sim$1 MPa when seeded with either cell type. Conversely, biochemical composition (proteoglycan and collagen content) increased steadily with culture duration, and was not dependent on the scaffold architecture. Histology of transverse sections showed cell infiltration into the outer two-third of the scaffold and increasing matrix deposition with time (not shown). The most interesting finding in this study was that while cells on NA and AL scaffolds produce similar amounts of ECM, marked increases in tensile properties were observed only on AL scaffolds. This finding may be explained by the organization of newly deposited ECM. On AL scaffolds, polarized light microscopy showed collagen deposition occurring in an ordered fashion, whereas deposited collagen was disorganized on NA scaffolds (Fig. 11). In related studies using MFCs derived from surgical waste tissue from 10 human donors,[104] similar results were observed, with tensile mechanical property increases correlating strongly with the amount of collagen deposition. Importantly, the stress–strain response of these MFC-seeded scaffolds from several donors matched that of the native meniscus in its normal operating range (0–6% strain). However, the long time required for cell colonization (42–70 days) and the need for space for robust matrix accumulation motivates our continued development of these novel scaffolds and culture systems (as described below).

Case example: annulus fibrosus

Another tissue of focus for nanofiber-based tissue engineering is the AF of the intervertebral disc. Like the meniscus, this tissue relies on an ordered collagen ultrastructure to impart defined mechanical function. Unlike the meniscus, the annulus is a laminate structure with alternating planes of organized fibers oriented at $\sim\pm30^\circ$ relative to the cross-sectional plane. Toward engineering a single annulus layer, we have tested rectangular samples removed from aligned fibrous meshes at angles that are not coincident to the fiber direction (Fig. 12A).[82] The mechanics of these acellular meshes were further characterized using a homogenization model that we have previously applied to native AF tissue, and we found good agreement between modeled and measured linear-region moduli.[82] In subsequent studies, AF cells isolated from bovine caudal discs were seeded onto scaffolds with fiber orientations of 0°, 30°, and 90° with respect to the longitudinal axis of the sample. These cell-laden constructs were cultured in a chemically defined serum-free growth media (as above) and mechanically tested at regular intervals. Histological and biochemical analyses were also carried out.

Results of this study showed that when seeded with AF cells, scaffolds increase in tensile moduli with time for each

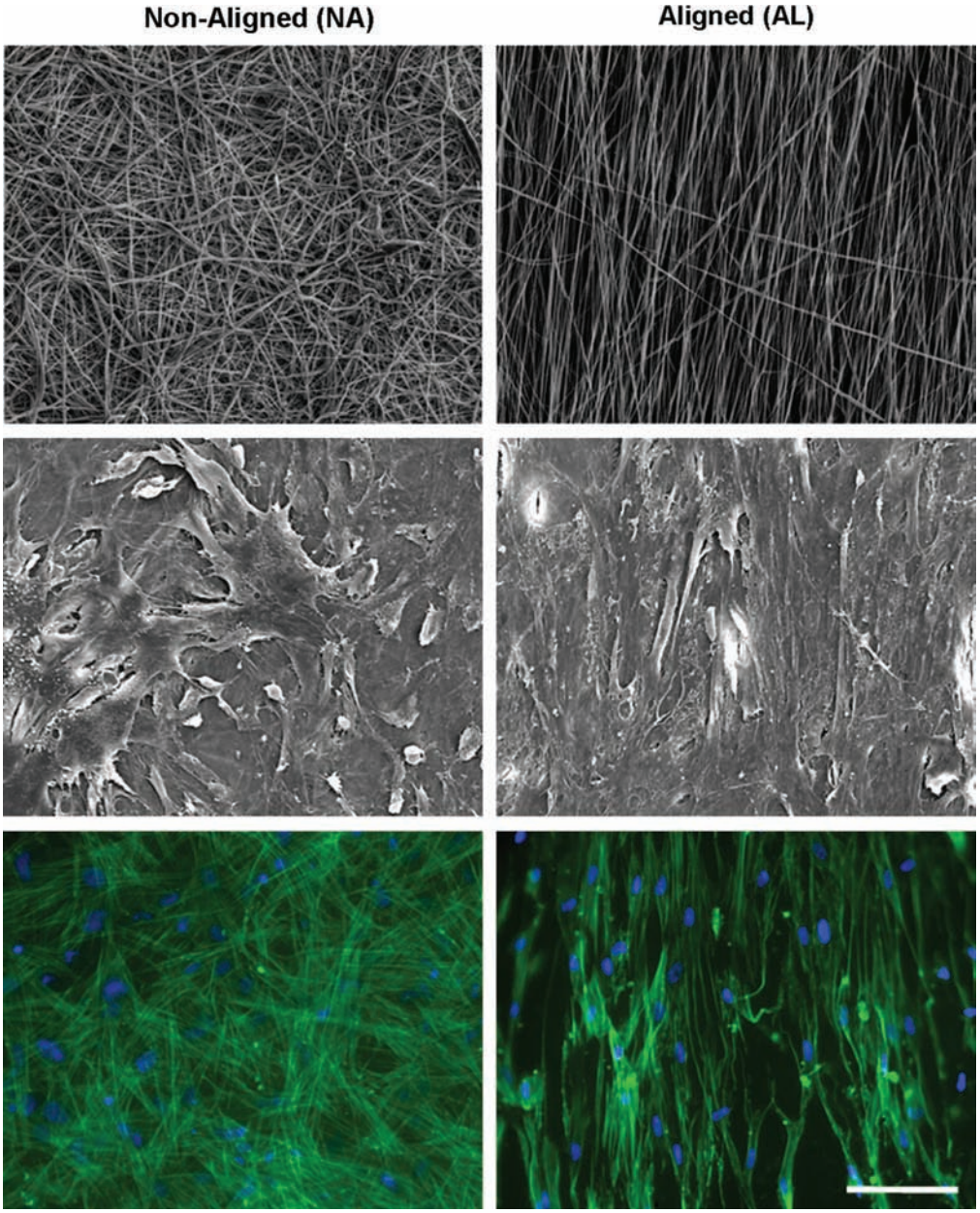

FIG. 10. Nanofibrous topography controls cell morphology. (Top row) Scanning electron micrographs of NA and AL electrospun PCL meshes. (Middle row) Scanning electron microscopy images of MSCs seeded on these meshes after 7 days of culture. Note that cell polarity is dictated by the underlying scaffold topography. (Bottom row) Actin staining (green, with DAPI [blue] nuclear counter stain) shows that cytoskeletal elements within cells are similarly organized to reflect the underlying topography. Scale bar = 50 μm. Color images available online at www.liebertonline.com/ten.

fiber orientation (Fig. 12C–E). Notably, constructs tested in the fiber direction ($\varphi = 0^\circ$) increased by $\sim$25 MPa (140%), while oblique ($\varphi = 30^\circ$) and transverse ($\varphi = 90^\circ$) constructs increased by $\sim$2 MPa (33–100%). These cell-seeded scaffolds with a fiber orientation similar to the AF ($\varphi = 30^\circ$) matched the circumferential linear region modulus of native inner AF (5.6 MPa) after just 8 weeks of culture (7.3 MPa). However, the $\varphi = 0^\circ$ fiber direction modulus (43.3 MPa) remains below the single lamella of the native AF (77.6 MPa).[115] The toe-region modulus in the fiber direction (9.1 MPa), however, was slightly higher than native AF (5.9 MPa). Therefore, in the range of small deformations, constructs achieved comparable tensile properties to native tissue by 8 weeks. As with meniscus constructs above, the orientation of deposited collagen coincided with the scaffold fiber direction (Fig. 12B).

Additionally, a fiber-reinforced constitutive model was applied to tensile stress–strain curves of these samples to yield four scalar material parameters with physically discrete meanings: μ, nonfibrillar (matrix) stiffness; ν, matrix compressibility; γ, fiber stiffness; ξ, fiber nonlinearity. When the hyperelastic model was applied, data from $\varphi = 90^\circ$ and $\varphi = 0^\circ$ samples fit well (Fig. 12F; $R^2 > 0.98$) and yielded excellent predictions for $\varphi = 30^\circ$ samples (not shown, $R^2 > 0.98$),

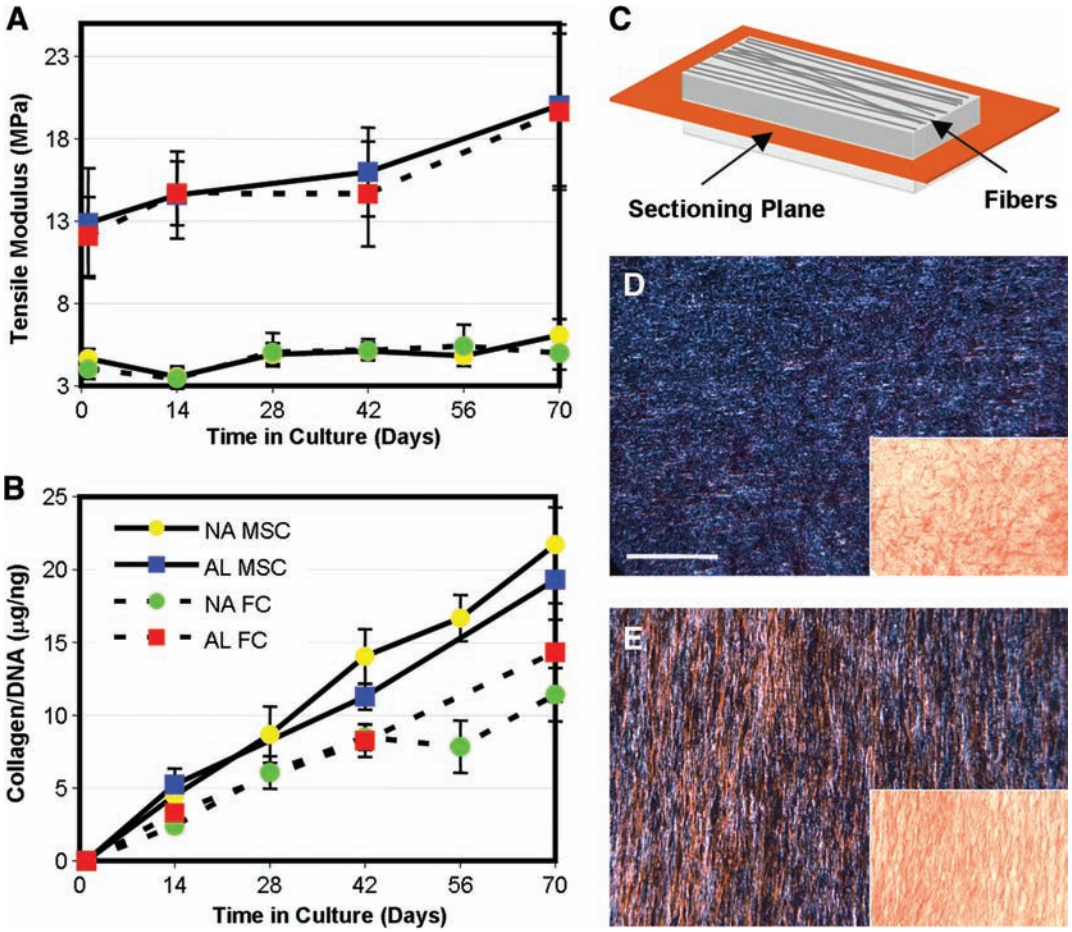

FIG. 11. Case example: meniscus tissue engineering. MSCs and MFCs were grown on either NA or AL PCL scaffolds for up to 10 weeks of *in vitro* culture. (**A**) On AL scaffolds, both MSC- and MFC-seeded constructs increased by ~10 MPa over this time course, while the same cells on NA scaffolds only increased by ~1 MPa. (**B**) Differential growth was not a function of ECM deposition, as similar amounts of collagen (as well as proteoglycan, not shown) were deposited in each scaffold. Producing *en face* sections (in the scaffold plane, (**C**) shown schematically) and viewing under polarized light (insets, **D** and **E**) show that organized collagen is present only in aligned scaffolds (**E**). Scale bar = 100 μm. Data adapted from Ref.[80] Color images available online at www.liebertonline.com/ten.

thereby validating the model for this application. The material parameters that represent the matrix (Fig. 12G) and fibers (Fig. 12H) increased with time in culture. Of these, the largest increase was for fiber stiffness γ, and these model parameters correlated well with biochemical content. These results suggest that the functional improvement of the constructs is based on the increasing contribution of fibrillar and matrix ECM. This work additionally confirmed the ability of AF cells to colonize and deposit organized, functional ECM, with similar composition and architecture as the native tissue. Further, this study demonstrates the utility of an approach that couples experimental measurement with constitutive modeling to characterize the full nonlinear behavior of constructs. This approach will help to elucidate the physical and biochemical mechanisms of functional growth and may help guide our tissue engineering efforts for creating functional AF tissue for implantation.

Other Considerations

While the results above clearly indicate the potential of nanofibrous scaffolds for soft tissue engineering, there remain a number of challenges and opportunities for advancement of the technology that should be addressed. Some of these issues are detailed below.

Enhancing cell infiltration

While cell-mediated matrix deposition can generate functional constructs, one significant limitation in engineering fibrous constructs for implantation is the long durations required for scaffold colonization of slow degrading aligned polyester scaffolds. This limits both the rate of matrix accumulation, as well as potentially limiting the degree to which integration with native structures can occur. As detailed above, using juvenile bovine and adult human MFCs, ~1-mm-thick scaffolds were only colonized in the peripheral two-thirds thickness after 10 weeks in culture.[80,104] It thus appears that these dense fibrous arrays, while providing a suitable micropattern for directing growth, can also be a physical impediment to cell infiltration. When formed into an aligned configuration, this issue is exacerbated as the apparent density in scaffolds is significantly increased compared to non-aligned or random scaffolds.[81]

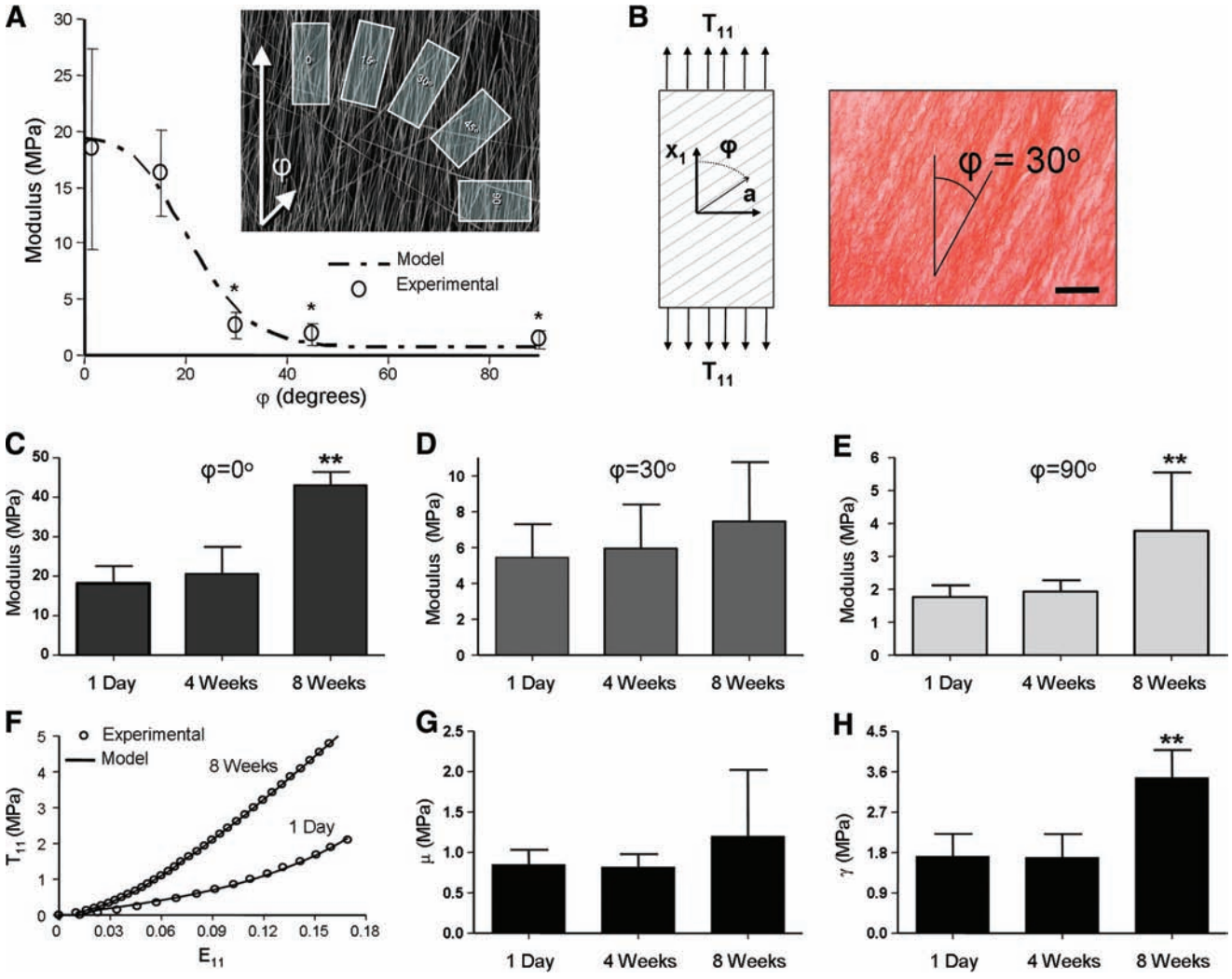

FIG. 12. Case example: AF tissue engineering. (**A**) Mechanical response and properties of acellular aligned scaffolds tested in directions that are not coincident (see inset) with the prevailing fiber direction can be captured with simple composite models. (**B**) When seeded with AF cells, matrix deposition (collagen staining) is coincident with the direction of the underlying fibers. Mechanical properties of cell-seeded scaffolds of different orientations (**C**: 0°, in fiber direction; **D**: 30°, off axis to the scaffold direction; **E**: 90°, perpendicular to the fiber direction) increase with time in culture. (**F**) Hyperelastic models capture the temporal evolution of functional matrix. Representative curves for engineered AF ($\varphi = 0^\circ$) demonstrate a nonlinear response in uniaxial tension. With time in culture, ECM deposition increases the nonlinearity and modulus from 1 day to 8 weeks. The model (solid lines) successfully fit experimental tensile behavior (open circles) at each time point, as shown. Model parameters for matrix (**G**) and fiber (**H**) moduli increase with culture duration. Data adapted from Ref.[82,112] Color images available online at www.liebertonline.com/ten.

While numerous potential solutions could be posited for overcoming this hurdle, ranging from fluid pressure[116] to galvanotactic mechanisms,[117] few reports exist on expedited infiltration. The most direct method for overcoming this barrier would be to place cells directly into the scaffold as it is formed. This has recently been accomplished by Stankus and co-workers, who electrosprayed cells in onto a common mandrel onto which PEUU fibers were simultaneously being collected.[118] This is an exciting new process, though scale-up and sterility may limit its wide-spread application. Another method for increasing cell infiltration may be to form ECM proteins directly into nanofiber form. Biologic elements (including collagen) provide a biomimetic environment for cell adhesion and thus are more readily colonized. Telemeco and colleagues reported enhanced cell infiltration into pure collagen scaffolds compared to synthetic scaffolds with subcutaneous implantation.[119] In these biologic scaffolds, cells may colonize by one of two routes, either through direct interaction in which they pull themselves through the proteinaceous milieu or they may degrade the ECM by secretion of matrix metalloproteinases. One drawback of this strategy, however, is that scaffolds mechanical properties using biologic polymers are considerably lower than that of common synthetic nanofibrous scaffolds,[51,96] and that pretreatment with crosslinking agents (such as gluteraldehyde) are required for their stabilization.

An alternative to these direct approaches can be found in the extensive literature on porous foams and sponges. From

that body of work, it appears that there exists an optimal pore size to promote cell infiltration.[120] For nanofibrous scaffolds, this approach has been addressed by mixing fibers of different diameters to limit fiber packing.[116] Alternatively, pores may be introduced by including salt particles at the time of production and subsequently leaching the salt out.[121] In the former case, some increase in cell infiltration was observed, particularly when coupled with fluid flow through the scaffold thickness. In the latter case, salt crystals created planes of separation within the scaffold into which cells could migrate, though this compromised the overall structural integrity of the scaffold. In place of salt, still others have induced the formation of ice crystals from relative humidity with collection on a super-cooled collecting surface to provide solid inclusions around which fibers form.[122] Still, others have simply increased the fiber size itself, transitioning from sub-micron-sized fibers to fibers on the order of tens of microns.[123] This approach increases cellular infiltration, but sacrifices the biomimetic characteristics of the nanofibrous topography. Such size increases in fiber size adversely impact cellular behavior.[40]

An alternative approach to these aforementioned techniques is to increase the size of the pores themselves, while not altering the nano-scale morphology of the fibers or the preinstilled fiber alignment. To achieve such a goal, Baker and co-workers have recently reported on a novel dual-electrospinning process in which two fiber populations are deposited onto a common rotating mandrel[93] (Fig. 13). By carefully selecting fabrication parameters and degree of overlap between spinnerets, one can control the relative fraction of each polymer in the resulting composite mesh. Inclusion of fiber populations that are rapidly eroding and/or soluble in aqueous solutions (such as PEO) dramatically enhances porosity as the sacrificial component elutes from the composite. Figure 13 shows an example of this process, where the interspersion of discrete fibers of differing composition is achieved and organized fiber directionality is maintained within the scaffold. As might be

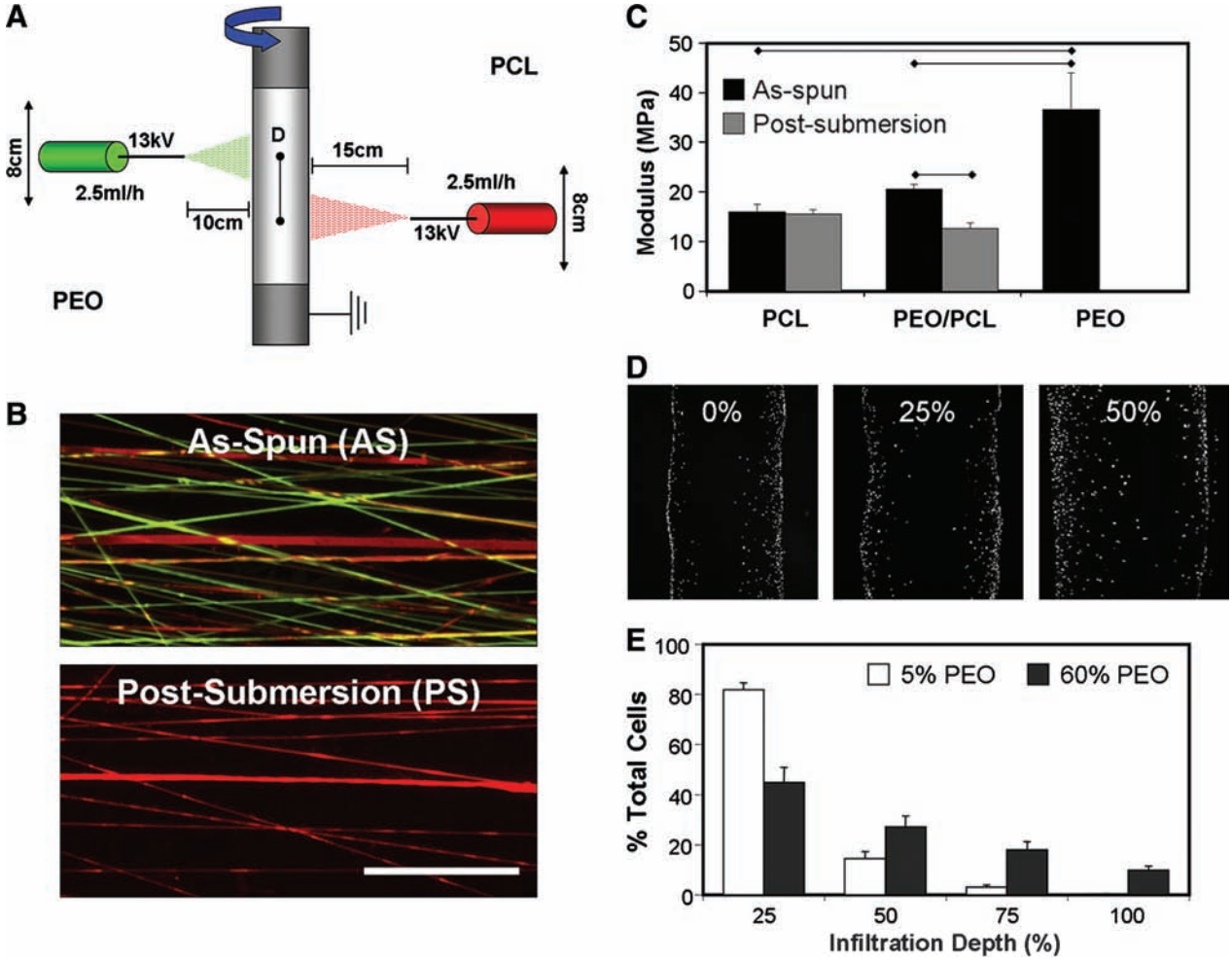

FIG. 13. Enhancing cell infiltration via the inclusion of sacrificial fibers. A dual electrospinning system (**A**) delivers two interspersed fiber populations to a common grounded rotating mandrel (red, PCL; green, PEO), and removal of the sacrificial component fibers (PEO) upon submersion in an aqueous environment (**B**). Mechanical properties of slowly degrading meshes, such as PCL, do not change with hydration, while pure sacrificial meshes degrade completely. Mixtures of PEO and PCL fibers decrease in mechanical properties after submersion (**C**). Increased porosity enhances infiltration of MSCs into the scaffold by week 3 of *in vitro* culture (**D**). Quantification shows increased fractions of sacrificial components (60%) led to increasing numbers of cells within the central region (50–100% infiltration depth) of the scaffold (**E**). Data adapted from Ref.[93] Color images available online at www.liebertonline.com/ten.

predicted, elution of sacrificial fibers from the composite has a pronounced effect on scaffold properties. Combining individual fiber components with dissimilar mechanical properties influences the composite scaffold mechanics, and does so as a function of the fiber fractions employed. Fiber mixing also alters several key features of the stress–strain profile, including the toe region and the plastic deformation response of the scaffolds after reaching their yield point. Both visual inspection and mechanical testing of scaffolds before and after removal of PEO fibers show that mechanical anisotropy was preserved. Further, by offsetting the source spinnerets with respect to one another, a graded fibrous mesh was produced with varying PEO contents. The tensile properties (maximum stress, stiffness, and modulus) reflected the amount of sacrificial component removed from the scaffold. When seeded with MSCs, scaffolds with greater amounts of removed sacrificial fibers showed pronounced increases in their cell infiltration rates.[93]

To further this area of inquiry, and to potentially offset the loss in properties with sacrificial fiber removal, we have recently adapted our techniques to allow for as many as three individual polymers to be spun simultaneously onto the same collecting mandrel[94] (Fig. 14). The mechanical properties of these multipolymer composites can be tuned to compensate for losses in properties from sacrificial fiber removal, such that cell ingress can be promoted despite the removal of a significant sacrificial fiber fraction.

Reconstituting anatomic form

Fabrication and maturation of a simple planar structure that recapitulates the primary mechanical features of the native tissue is a considerable challenge. Added to this is the fact that most tissues possess a specific anatomic form, and in some tissues, such as the intervertebral disc and meniscus, this form is a critical component of tissue function. Most nanofibrous scaffolds begin as flat sheets or hollow tubes (when collected on a mandrel). This latter form is particularly useful for small blood vessel tissue engineering, and unique multilayered tissues have been formed using this technique.[90] For other more complicated structures, few construction algorithms exist. Recent reports show that an MSC-seeded

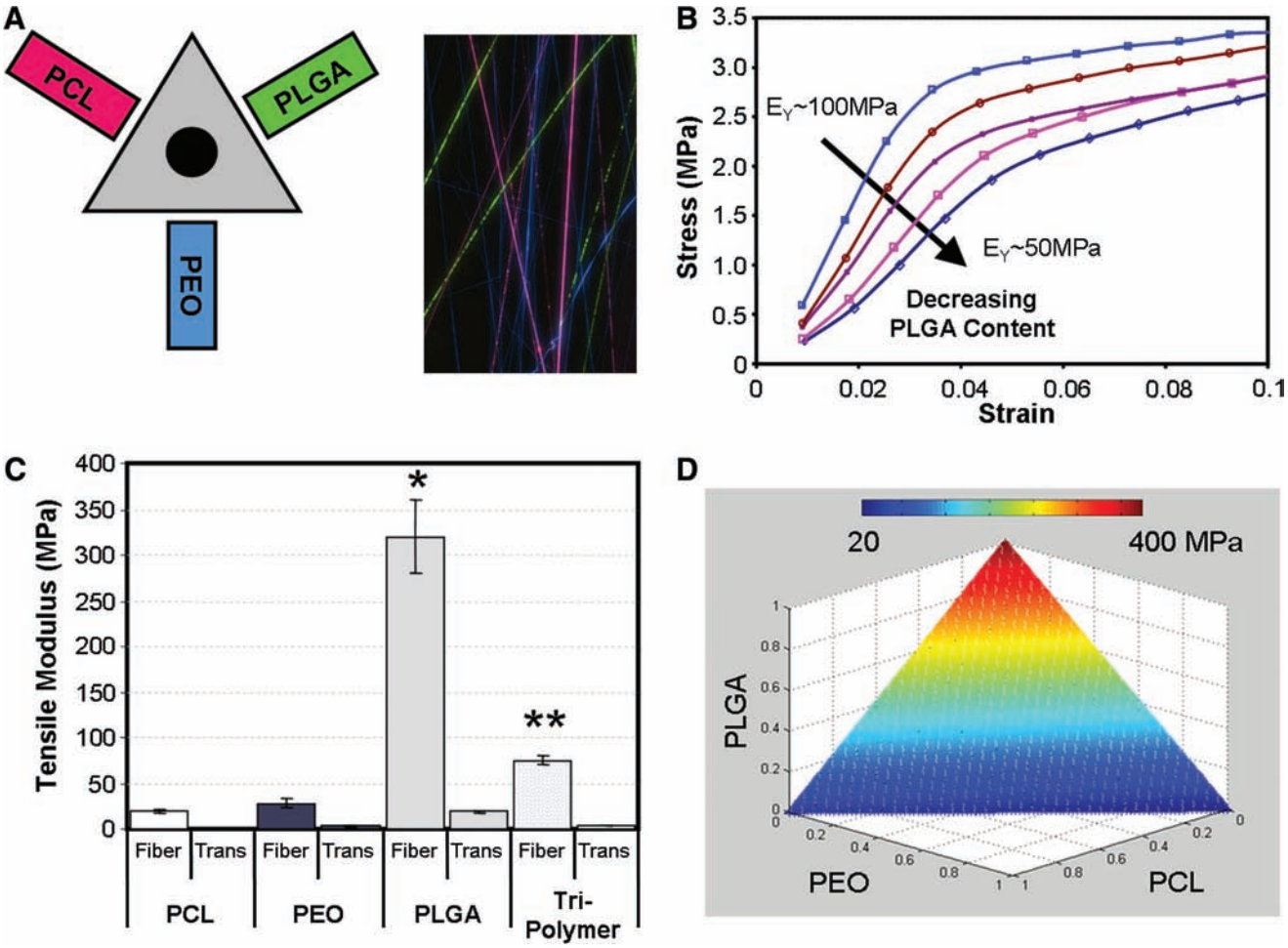

FIG. 14. Multipolymer nanofibrous composites. Scaffold mechanics can be tuned with the integration of different polymers into nanofibrous composites. Here three polymers [PEO, PCL, and poly(D,L-lactide-co-glycolide)] were collected simultaneously to produce a fully interspersed fiber mixture (**A**). Changing component ratios affects the resulting stress–strain response (**B**). Mechanical properties of the composite are dictated by the relative fraction of each constituent (**C**). Using this approach, and based on the starting properties of each individual polymer, a wide range of scaffold properties can be generated (**D**). Data adapted from Ref.[94] Color images available online at www.liebertonline.com/ten.

nanofibrous scaffold can be press-fit into a molding apparatus, and maintain their form for up to 6 weeks of *in vitro* rotating wall bioreactor culture.[124] Others have investigated multicomponent scaffolds, where a gelatinous core is established (by injection) in the mid-substance of a nanofibrous sheet for intervertebral disc applications.[125] Still others have begun to investigate how layers of nanofibers can be seeded with cells, and then stacked to achieve anatomic forms such as periodontal ligament[126] as well as more complicated structures recreating the anatomic form of the IVD and the knee meniscus[127,128] (Fig. 15).

Conclusions and Future Directions

The large body of literature that has recently emerged concerning nanofibrous scaffolds is a testament to the degree of excitement in the field regarding their potential for tissue engineering applications. As the field advances, several exciting new possibilities arise, and what first emerged as a simple straight-and-narrow template for organizing cells will develop into multifunctional scaffolds that enhance tissue repair and regeneration. Emerging work focused on the combination of multiple polymers into composite arrays will

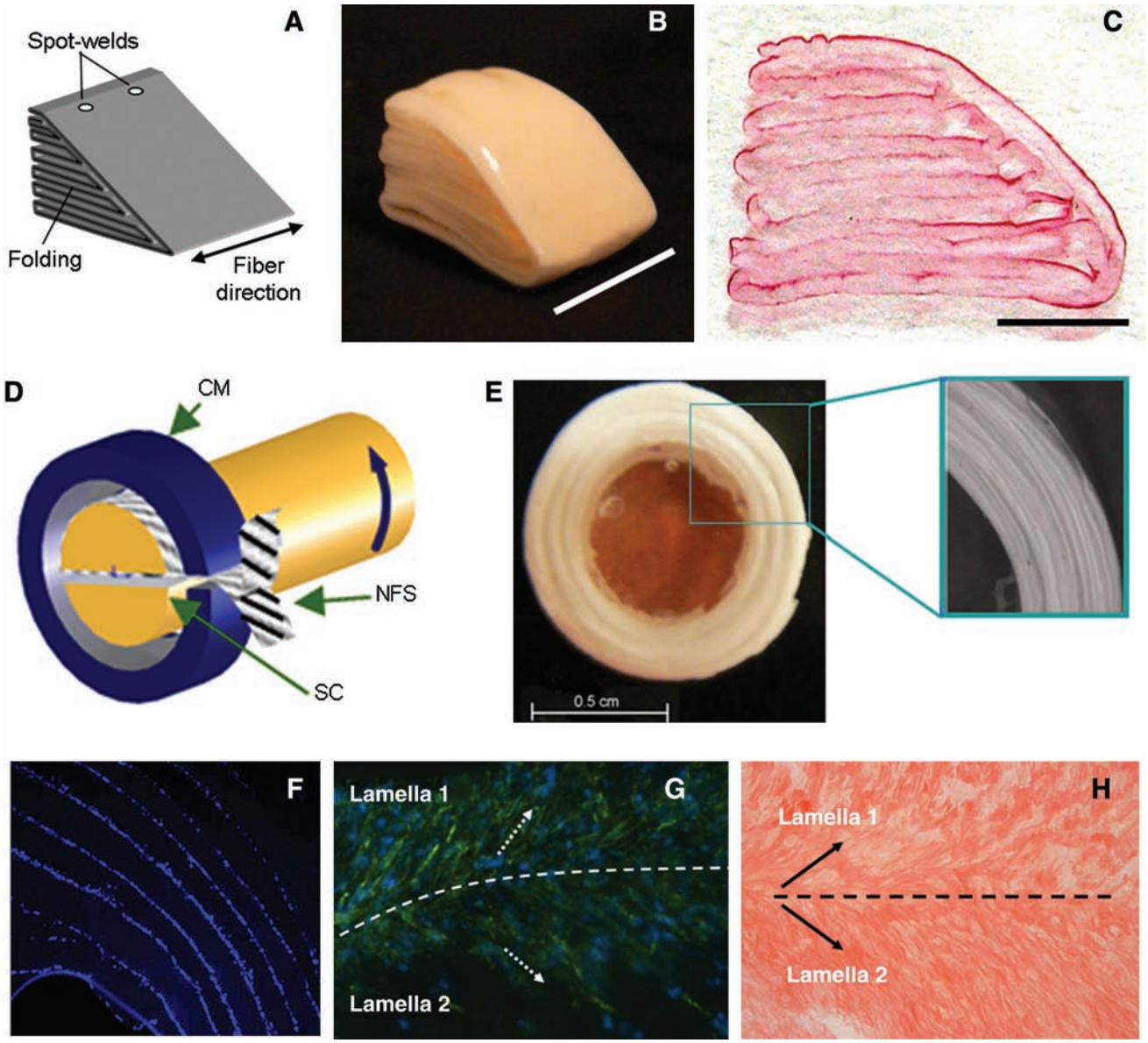

FIG. 15. Engineering anatomic form with nanofibrous scaffolds. Nanofibrous scaffolds are typically formed as planar samples, while most fiber-reinforced tissues have specialized anatomic form. For complex structures, such as the knee meniscus (**A–C**) and the intervertebral disc (**D–H**), construction algorithms must be developed for *in vivo* application. Custom wrapping can produce cell-laden wedge-shaped structures for meniscus applications (**B**) that can be colonized by seeded cells (**C**). For IVD, annular composites with multiple layers can be formed (**D, E**). Cell-seeded IVD composites localize cells to lamellar interfaces (**F**), and direct cell (**G**) and matrix (**H**) organization in each layer. Color images available online at www.liebertonline.com/ten.

allow for the tuning of scaffold properties to match those of numerous native tissues.[34,94] New drug and gene delivery methods are emerging that will impart additional functionality,[129–131] potentially improving *in vivo* maturation rates and expanding the potential clinical application. Bioreactor systems that promote tissue growth via nutrient provision[132] and/or mechanical stimulation[133] will increasingly be utilized to foster nanofiber-based tissue development. Further, consideration of soft–hard interfaces, such as tendon insertion sites,[134] may be addressed via selective induction of mineralization and bone formation with inclusion of hydroxyapatite crystals.[135] As these developments occur and, in particular, as advances are made in the area of load-bearing tissue engineering, special attention must be given to the appropriate characterization methods and analysis of mechanical properties of these unique scaffolds. Moreover, production methods must be optimized, such that nanofibrous scaffold production is less of an art, and more of a science. For this, we must endeavor toward higher throughput production methods, and the establishment of good manufacturing protocols and rigorous analyses. Finally, we must ultimately test these scaffolds in realistic and challenging load-bearing situations to evaluate their *in vivo* efficacy.[136] These include the tensile loading methods described in this review, as well as compressive testing modalities (including equilibrium and dynamic testing) when implants are to be used in compressive and or mixed load-bearing situations (e.g., in the knee meniscus). Taken together, this unique approach for the multiscale rendering of fiber reinforcement from the nano- and micron-levels holds tremendous potential for the repair or replacement of fiber-reinforced tissues.

Acknowledgments

Funding for this work was provided by the National Institutes of Health (RO1 EB02425), the Aircast Foundation, The NFL charities, and the Penn Center of Musculoskeletal Disorders (P30 AR050950). The authors would like to acknowledge Ms. Lara Ionescu for provision of the fetal and adult meniscus images and Mr. Ashwin Nathan for strain maps of deformed scaffolds.

Disclosure Statement

No competing financial interests exist.

References

1. Lynch, H.A., Johannessen, W., Wu, J.P., Jawa, A., and Elliott, D.M. Effect of fiber orientation and strain rate on the nonlinear uniaxial tensile material properties of tendon. J Biomech Eng **125,** 726, 2003.
2. Setton, L.A., Guilak, F., Hsu, E.W., and Vail, T.P. Biomechanical factors in tissue engineered meniscal repair. Clin Orthop **367 Suppl,** S254, 1999.
3. Holzapfel, G.A., Schulze-Bauer, C.A., Feigl, G., and Regitnig, P. Single lamellar mechanics of the human lumbar anulus fibrosus. Biomech Model Mechanobiol **3,** 125, 2005.
4. Proctor, C.S., Schmidt, M.B., Whipple, R.R., Kelly, M.A., and Mow, V.C. Material properties of the normal medial bovine meniscus. J Orthop Res **7,** 771, 1989.
5. Hayes, A.J., Benjamin, M., and Ralphs, J.R. Extracellular matrix in development of the intervertebral disc. Matrix Biol **20,** 107, 2001.
6. Clark, C.R., and Ogden, J.A. Development of the menisci of the human knee joint. Morphological changes and their potential role in childhood meniscal injury. J Bone Joint Surg Am **65,** 538, 1983.
7. Beredjiklian, P.K., Favata, M., Cartmell, J.S., Flanagan, C.L., Crombleholme, T.M., and Soslowsky, L.J. Regenerative versus reparative healing in tendon: a study of biomechanical and histological properties in fetal sheep. Ann Biomed Eng **31,** 1143, 2003.
8. Wang, J.H., Jia, F., Gilbert, T.W., and Woo, S.L. Cell orientation determines the alignment of cell-produced collagenous matrix. J Biomech **36,** 97, 2003.
9. Frank, C.B., and Jackson, D.W. The science of reconstruction of the anterior cruciate ligament. J Bone Joint Surg Am **79,** 1556, 1997.
10. Greis, P.E., Bardana, D.D., Holmstrom, M.C., and Burks, R.T. Meniscal injury: I. Basic science and evaluation. J Am Acad Orthop Surg **10,** 168, 2002.
11. Asch, H.L., Lewis, P.J., Moreland, D.B., Egnatchik, J.G., Yu, Y.J., Clabeaux, D.E., and Hyland, A.H. Prospective multiple outcomes study of outpatient lumbar microdiscectomy: should 75 to 80% success rates be the norm? J Neurosurg **96,** 34, 2002.
12. Koebbe, C.J., Maroon, J.C., Abla, A., El-Kadi, H., and Bost, J. Lumbar microdiscectomy: a historical perspective and current technical considerations. Neurosurg Focus **13,** E3, 2002.
13. Newman, A.P., Anderson, D.R., Daniels, A.U., and Dales, M.C. Mechanics of the healed meniscus in a canine model. Am J Sports Med **17,** 164, 1989.
14. Provenzano, P.P., Hurschler, C., and Vanderby, R., Jr. Microstructural morphology in the transition region between scar and intact residual segments of a healing rat medial collateral ligament. Connect Tissue Res **42,** 123, 2001.
15. Matsumoto, N., Horibe, S., Nakamura, N., Senda, T., Shino, K., and Ochi, T. Effect of alignment of the transplanted graft extracellular matrix on cellular repopulation and newly synthesized collagen. Arch Orthop Trauma Surg **117,** 215, 1998.
16. Schoderbek, R.J., Jr., Treme, G.P., and Miller, M.D. Bone-patella tendon-bone autograft anterior cruciate ligament reconstruction. Clin Sports Med **26,** 525, 2007.
17. Arnoczky, S.P., DiCarlo, E.F., O'Brien, S.J., and Warren, R.F. Cellular repopulation of deep-frozen meniscal autografts: an experimental study in the dog. Arthroscopy **8,** 428, 1992.
18. Butler, D.L., Shearn, J.T., Juncosa, N., Dressler, M.R., and Hunter, S.A. Functional tissue engineering parameters toward designing repair and replacement strategies. Clin Orthop Relat Res **427 Suppl,** S190, 2004.
19. Awad, H.A., Butler, D.L., Harris, M.T., Ibrahim, R.E., Wu, Y., Young, R.G., Kadiyala, S., and Boivin, G.P. *In vitro* characterization of mesenchymal stem cell-seeded collagen scaffolds for tendon repair: effects of initial seeding density on contraction kinetics. J Biomed Mater Res **51,** 233, 2000.
20. Garvin, J., Qi, J., Maloney, M., and Banes, A.J. Novel system for engineering bioartificial tendons and application of mechanical load. Tissue Eng **9,** 967, 2003.
21. Costa, K.D., Lee, E.J., and Holmes, J.W. Creating alignment and anisotropy in engineered heart tissue: role of boundary conditions in a model three-dimensional culture system. Tissue Eng **9,** 567, 2003.
22. Barocas, V.H., Girton, T.S., and Tranquillo, R.T. Engineered alignment in media equivalents: magnetic prealignment and mandrel compaction. J Biomech Eng **120,** 660, 1998.

23. Altman, G.H., Horan, R.L., Lu, H.H., Moreau, J., Martin, I., Richmond, J.C., and Kaplan, D.L. Silk matrix for tissue engineered anterior cruciate ligaments. Biomaterials **23,** 4131, 2002.
24. Cooper, J.A., Lu, H.H., Ko, F.K., Freeman, J.W., and Laurencin, C.T. Fiber-based tissue-engineered scaffold for ligament replacement: design considerations and *in vitro* evaluation. Biomaterials **26,** 1523, 2005.
25. Cooper, J.A., Jr., Sahota, J.S., Gorum, W.J., 2nd, Carter, J., Doty, S.B., and Laurencin, C.T. Biomimetic tissue-engineered anterior cruciate ligament replacement. Proc Natl Acad Sci USA **104,** 3049, 2007.
26. Horan, R.L., Collette, A.L., Lee, C., Antle, K., Chen, J., and Altman, G.H. Yarn design for functional tissue engineering. J Biomech **39,** 2232, 2006.
27. Moutos, F.T., Freed, L.E., and Guilak, F. A biomimetic three-dimensional woven composite scaffold for functional tissue engineering of cartilage. Nat Mater **6,** 162, 2007.
28. Formhals, A. Process and apparatus for preparing artificial threads. 1934, United States Patent Office. Patent no. 1,975,504.
29. Burger, C., Hsiao, B.S., and Chu, B. Nanofibrous materials and their applications. Annu Rev Mater Res **36,** 333, 2006.
30. Li, W.J., Mauck, R.L., and Tuan, R.S. Electrospun nanofibrous scaffolds: production, characterization, and applications for tissue engineering and drug delivery. J Biomed Nanotechnol **1,** 259, 2005.
31. Teo, W.E., and Ramakrishna, S. A review on electrospinning design and nanofibre assemblies. Nanotechnology **17,** R89, 2006.
32. Li, D., and Xia, Y.N. Electrospinning of nanofibers: reinventing the wheel? Adv Mater **16,** 1151, 2004.
33. Pham, Q.P., Sharma, U., and Mikos, A.G. Electrospinning of polymeric nanofibers for tissue engineering applications: a review. Tissue Eng **12,** 1197, 2006.
34. Barnes, C.P., Sell, S.A., Boland, E.D., Simpson, D.G., and Bowlin, G.L. Nanofiber technology: designing the next generation of tissue engineering scaffolds. Adv Drug Deliv Rev **59,** 1413, 2007.
35. Shin, Y.M., Hohman, M.M., Brenner, M.P., and Rutledge, G.C. Experimental characterization of electrospinning: the electrically forced jet and instabilities. Polymer **42,** 9955, 2001.
36. Reneker, D.H., and Chun, I. Nanometre diameter fibres of polymer, produced by electrospinning. Nanotechnology **7,** 216, 1996.
37. Deitzel, J.M., Kleinmeyer, J., Harris, D., and Beck Tan, N.C. The effect of processing variables on the morphology of electrospun nanofibers and textiles. Polymer **42,** 261, 2001.
38. Riesle, J., Hollander, A.P., Langer, R., Freed, L.E., and Vunjak-Novakovic, G. Collagen in tissue-engineered cartilage: types, structure, and crosslinks. J Cell Biochem **71,** 313, 1998.
39. Nur, E.K.A., Ahmed, I., Kamal, J., Schindler, M., and Meiners, S. Three dimensional nanofibrillar surfaces induce activation of Rac. Biochem Biophys Res Commun **331,** 428, 2005.
40. Li, W.J., Jiang, Y.J., and Tuan, R.S. Chondrocyte phenotype in engineered fibrous matrix is regulated by fiber size. Tissue Eng **12,** 1775, 2006.
41. Li, W.J., Laurencin, C.T., Caterson, E.J., Tuan, R.S., and Ko, F.K. Electrospun nanofibrous structure: a novel scaffold for tissue engineering. J Biomed Mater Res **60,** 613, 2002.
42. Khil, M.S., Cha, D.I., Kim, H.Y., Kim, I.S., and Bhattarai, N. Electrospun nanofibrous polyurethane membrane as wound dressing. J Biomed Mater Res B Appl Biomater **67,** 675, 2003.
43. Xu, C., Inai, R., Kotaki, M., and Ramakrishna, S. Electrospun nanofiber fabrication as synthetic extracellular matrix and its potential for vascular tissue engineering. Tissue Eng **10,** 1160, 2004.
44. Venugopal, J., Ma, L.L., Yong, T., and Ramakrishna, S. *In vitro* study of smooth muscle cells on polycaprolactone and collagen nanofibrous matrices. Cell Biol Int **29,** 861, 2005.
45. Yoshimoto, H., Shin, Y.M., Terai, H., and Vacanti, J.P. A biodegradable nanofiber scaffold by electrospinning and its potential for bone tissue engineering. Biomaterials **24,** 2077, 2003.
46. Boland, E.D., Telemeco, T.A., Simpson, D.G., Wnek, G.E., and Bowlin, G.L. Utilizing acid pretreatment and electrospinning to improve biocompatibility of poly(glycolic acid) for tissue engineering. J Biomed Mater Res B Appl Biomater **71,** 144, 2004.
47. Yang, F., Murugan, R., Wang, S., and Ramakrishna, S. Electrospinning of nano/micro scale poly(L-lactic acid) aligned fibers and their potential in neural tissue engineering. Biomaterials **26,** 2603, 2005.
48. Yang, F., Xu, C.Y., Kotaki, M., Wang, S., and Ramakrishna, S. Characterization of neural stem cells on electrospun poly(L-lactic acid) nanofibrous scaffold. J Biomater Sci Polym Ed **15,** 1483, 2004.
49. Li, W.J., Cooper, J.A., Jr., Mauck, R.L., and Tuan, R.S. Fabrication and characterization of six electrospun poly(alpha-hydroxy ester)-based fibrous scaffolds for tissue engineering applications. Acta Biomater **2,** 377, 2006.
50. Boland, E.D., Coleman, B.D., Barnes, C.P., Simpson, D.G., Wnek, G.E., and Bowlin, G.L. Electrospinning polydioxanone for biomedical applications. Acta Biomater **1,** 115, 2005.
51. Matthews, J.A., Wnek, G.E., Simpson, D.G., and Bowlin, G.L. Electrospinning of collagen nanofibers. Biomacromolecules **3,** 232, 2002.
52. Rho, K.S., Jeong, L., Lee, G., Seo, B.M., Park, Y.J., Hong, S.D., Roh, S., Cho, J.J., Park, W.H., and Min, B.M. Electrospinning of collagen nanofibers: effects on the behavior of normal human keratinocytes and early-stage wound healing. Biomaterials **27,** 1452, 2006.
53. Buttafoco, L., Kolkman, N.G., Engbers-Buijtenhuijs, P., Poot, A.A., Dijkstra, P.J., Vermes, I., and Feijen, J. Electrospinning of collagen and elastin for tissue engineering applications. Biomaterials **27,** 724, 2006.
54. Li, M., Mondrinos, M.J., Gandhi, M.R., Ko, F.K., Weiss, A.S., and Lelkes, P.I. Electrospun protein fibers as matrices for tissue engineering. Biomaterials **26,** 5999, 2005.
55. Min, B.M., Jeong, L., Nam, Y.S., Kim, J.M., Kim, J.Y., and Park, W.H. Formation of silk fibroin matrices with different texture and its cellular response to normal human keratinocytes. Int J Biol Macromol **34,** 281, 2004.
56. Min, B.M., Lee, G., Kim, S.H., Nam, Y.S., Lee, T.S., and Park, W.H. Electrospinning of silk fibroin nanofibers and its effect on the adhesion and spreading of normal human keratinocytes and fibroblasts *in vitro.* Biomaterials **25,** 1289, 2004.
57. Geng, X., Kwon, O.H., and Jang, J. Electrospinning of chitosan dissolved in concentrated acetic acid solution. Biomaterials **26,** 5427, 2005.
58. Bhattarai, N., Edmondson, D., Veiseh, O., Matsen, F.A., and Zhang, M. Electrospun chitosan-based nanofibers and their cellular compatibility. Biomaterials **26,** 6176, 2005.
59. Jiang, H., Fang, D., Hsiao, B.S., Chu, B., and Chen, W. Optimization and characterization of dextran membranes prepared by electrospinning. Biomacromolecules **5,** 326, 2004.

60. Woerdeman, D.L., Ye, P., Shenoy, S., Parnas, R.S., Wnek, G.E., and Trofimova, O. Electrospun fibers from wheat protein: investigation of the interplay between molecular structure and the fluid dynamics of the electrospinning process. Biomacromolecules **6,** 707, 2005.
61. Lee, S.J., Yoo, J.J., Lim, G.J., Atala, A., and Stitzel, J. *In vitro* evaluation of electrospun nanofiber scaffolds for vascular graft application. J Biomed Mater Res A **83,** 999, 2007.
62. Stitzel, J., Liu, J., Lee, S.J., Komura, M., Berry, J., Soker, S., Lim, G., Van Dyke, M., Czerw, R., Yoo, J.J., and Atala, A. Controlled fabrication of a biological vascular substitute. Biomaterials **27,** 1088, 2006.
63. Sell, S.A., McClure, M.J., Barnes, C.P., Knapp, D.C., Walpoth, B.H., Simpson, D.G., and Bowlin, G.L. Electrospun polydioxanone-elastin blends: potential for bioresorbable vascular grafts. Biomed Mater **1,** 72, 2006.
64. Casper, C.L., Yamaguchi, N., Kiick, K.L., and Rabolt, J.F. Functionalizing electrospun fibers with biologically relevant macromolecules. Biomacromolecules **6,** 1998, 2005.
65. Casper, C.L., Yang, W., Farach-Carson, M.C., and Rabolt, J.F. Coating electrospun collagen and gelatin fibers with perlecan domain I for increased growth factor binding. Biomacromolecules **8,** 1116, 2007.
66. Ma, Z., He, W., Yong, T., and Ramakrishna, S. Grafting of gelatin on electrospun poly(caprolactone) nanofibers to improve endothelial cell spreading and proliferation and to control cell orientation. Tissue Eng **11,** 1149, 2005.
67. Pornsopone, V., Supaphol, P., Rangkupan, R., and Tantayanon, S. Electrospinning of methacrylate-based copolymers: effects of solution concentration and applied electrical potential on morphological appearance of as-spun fibers. Polym Eng Sci **45,** 1073, 2005.
68. Kim, S.H., Nair, S., and Moore, E. Reactive electrospinning of cross-linked poly(2-hydroxyethyl methacrylate) nanofibers and elastic properties of individual hydrogel nanofibers in aqueous solutions. Macromolecules **38,** 3719, 2005.
69. Tan, A.R., Ifkovits, J.L., Baker, B.M., Brey, D.M., Mauck, R.L., and Burdick, J.A. Electrospinning of photocrosslinked and degradable fibrous scaffolds. J Biomed Mater Res A **87A,** 1034, 2008.
70. Ifkovits, J.L., Padera, R.F., and Burdick, J.A. Biodegradable and radically polymerized elastomers with enhanced processing capabilities. Biomed Mater **3,** 034104, 2008.
71. Fridrikh, S.V., Yu, J.H., Brenner, M.P., and Rutledge, G.C. Controlling the fiber diameter during electrospinning. Phys Rev Lett **90,** 144502, 2003.
72. Kidoaki, S., Kwon, I.K., and Matsuda, T. Structural features and mechanical properties of *in situ*-bonded meshes of segmented polyurethane electrospun from mixed solvents. J Biomed Mater Res B Appl Biomater **76,** 219, 2006.
73. Zhang, X., Thomas, V., and Vohra, Y.K. *In vitro* biodegradation of designed tubular scaffolds of electrospun protein/polyglyconate blend fibers. J Biomed Mater Res B Appl Biomater **89,** 135, 2008.
74. Theron, A., Zussman, E., and Yarin, A.L. Electrostatic field-assisted alignment of electrospun nanofibres. Nanotechnology **12,** 384, 2001.
75. Li, D., Ouyang, G., McCann, J.T., and Xia, Y. Collecting electrospun nanofibers with patterned electrodes. Nano Lett **5,** 913, 2005.
76. Li, D., Wang, Y.L., and Xia, Y.N. Electrospinning nanofibers as uniaxially aligned arrays and layer-by-layer stacked films. Adv Mater **16,** 361, 2004.
77. Sun, D., Chang, C., Li, S., and Lin, L. Near-field electrospinning. Nano Lett **6,** 839, 2006.
78. Sundaray, B., Subramanian, V., Natarajan, T.S., Xiang, R.Z., Chang, C.C., and Fann, W.S. Electrospinning of continuous aligned polymer fibers. Appl Phys Lett **84,** 1222, 2004.
79. Boland, E.D., Wnek, G.E., Simpson, D.G., Pawlowski, K.J., and Bowlin, G.L. Tailoring tissue engineering scaffolds using electrostatic processing techniques: a study of poly (glycolic acid) electrospinning. J Macromol Sci A **38,** 1231, 2001.
80. Baker, B.M., and Mauck, R.L. The effect of nanofiber alignment on the maturation of engineered meniscus constructs. Biomaterials **28,** 1967, 2007.
81. Li, W.J., Mauck, R.L., Cooper, J.A., Yuan, X., and Tuan, R.S. Engineering controllable anisotropy in electrospun biodegradable nanofibrous scaffolds for musculoskeletal tissue engineering. J Biomech **40,** 1686, 2007.
82. Nerurkar, N.L., Elliott, D.M., and Mauck, R.L. Mechanics of oriented electrospun nanofibrous scaffolds for annulus fibrosus tissue engineering. J Orthop Res **25,** 1018, 2007.
83. Courtney, T., Sacks, M.S., Stankus, J., Guan, J., and Wagner, W.R. Design and analysis of tissue engineering scaffolds that mimic soft tissue mechanical anisotropy. Biomaterials **27,** 3631, 2006.
84. Ayres, C., Bowlin, G.L., Henderson, S.C., Taylor, L., Shultz, J., Alexander, J., Telemeco, T.A., and Simpson, D.G. Modulation of anisotropy in electrospun tissue-engineering scaffolds: analysis of fiber alignment by the fast Fourier transform. Biomaterials **27,** 5524, 2006.
85. Kowalewski, T.A., Blonski, S., and Barral, S. Experiments and modelling of electrospinning process. Bull Pol Acad Sci Tech Sci **53,** 385, 2005.
86. Dosunmu, O.O., Chase, G.G., Kataphinan, W., and Reneker, D.H. Electrospinning of polymer nanofibres from multiple jets on a porous tubular surface. Nanotechnology **17,** 1123, 2006.
87. Theron, S.A., Yarin, A.L., Zussman, E., and Kroll, E. Multiple jets in electrospinning: experiment and modeling. Polymer **46,** 2889, 2005.
88. Yarin, A.L., and Zussman, E. Upward needleless electrospinning of multiple nanofibers. Polymer **45,** 2977, 2004.
89. Ding, B., Kimura, E., Sato, T., Fujita, S., and Shiratori, S. Fabrication of blend biodegradable nanofibrous nonwoven mats via multi-jet electrospinning. Polymer **45,** 1895, 2004.
90. Kidoaki, S., Kwon, I.K., and Matsuda, T. Mesoscopic spatial designs of nano- and microfiber meshes for tissue-engineering matrix and scaffold based on newly devised multilayering and mixing electrospinning techniques. Biomaterials **26,** 37, 2005.
91. Kwon, I.K., Kidoaki, S., and Matsuda, T. Electrospun nano- to microfiber fabrics made of biodegradable copolyesters: structural characteristics, mechanical properties and cell adhesion potential. Biomaterials **26,** 3929, 2005.
92. Madhugiri, S., Dalton, A., Gutierrez, J., Ferraris, J.P., and Balkus, K.J., Jr. Electrospun MEH-PPV/SBA-15 composite nanofibers using a dual syringe method. J Am Chem Soc **125,** 14531, 2003.
93. Baker, B.M., Gee, A.O., Metter, R.B., Nathan, A.S., Marklein, R.A., Burdick, J.A., and Mauck, R.L. The potential to improve cell infiltration in composite fiber-aligned electrospun scaffolds by the selective removal of sacrificial fibers. Biomaterials **29,** 2348, 2008.
94. Baker, B.M., Nerurkar, N.L., Burdick, J.A., Elliott, D.M., and Mauck, R.L. Fabrication and modeling of dynamic

multi-component nanofibrous scaffolds. J Biomech Eng 2008 (in review).
95. Shields, K.J., Beckman, M.J., Bowlin, G.L., and Wayne, J.S. Mechanical properties and cellular proliferation of electrospun collagen type II. Tissue Eng **10,** 1510, 2004.
96. Barnes, C.P., Pemble, C.W., Brand, D.D., Simpson, D.G., and Bowlin, G.L. Cross-linking electrospun type II collagen tissue engineering scaffolds with carbodiimide in ethanol. Tissue Eng **13,** 1593, 2007.
97. Tan, E.P., Ng, S.Y., and Lim, C.T. Tensile testing of a single ultrafine polymeric fiber. Biomaterials **26,** 1453, 2005.
98. Chew, S.Y., Hufnagel, T.C., Lim, C.T., and Leong, K.W. Mechanical properties of single electrospun drug-encapsulated nanofibres. Nanotechnology **17,** 3880, 2006.
99. Lim, C.T., Tan, E.P.S., and Ng, S.Y. Effects of crystalline morphology on the tensile properties of electrospun polymer nanofibers. Appl Phys Lett **92,** 141908, 2008.
100. Tan, E.P.S., Goh, C.N., Sow, C.H., and Lim, C.T. Tensile test of a single nanofiber using an atomic force microscope tip. Appl Phys Lett **86,** 073115, 2005.
101. Tan, E.P.S., and Lim, C.T. Effects of annealing on the structural and mechanical properties of electrospun polymeric nanofibres. Nanotechnology **17,** 2649, 2006.
102. Naraghi, M., Chasiotis, I., Kahn, H., Wen, Y., and Dzenis, Y. Novel method for mechanical characterization of polymeric nanofibers. Rev Sci Instrum **78,** 095108, 2007.
103. Naraghi, M., Chasiotis, I., Kahn, H., Wen, Y.K., and Dzenis, Y. Mechanical deformation and failure of electrospun polyacrylonitrile nanofibers as a function of strain rate. Appl Phys Lett **91,** 151901, 2007.
104. Baker, B.M., Nathan, A.S., Huffman, G.R., and Mauck, R.L. Tissue engineering with meniscus cells derived from surgical debris. Osteoarthritis Cartilage **17,** 336, 2009.
105. O'Connell, G.D., Sen, S., Baker, B.M., Mauck, R.L., and Elliott, D.M. Biaxial mechanics for muscoloskeletal tissue and fiber-reinforced scaffolds. Proceedings of BIO2007 Summer Bioengineering Conference, Keystone, CO. 2007.
106. Baker, B.M., O'Connell, G.D., Sen, S., Nathan, A.S., Elliott, D.M., and Mauck, R.L. Multi-lamellar and multi-axial maturation of cell-seeded fiber-reinforced tissue engineered constructs. Proceedings of BIO2007 Summer Bioengineering Conference, Keystone, CO. 2007.
107. Stella, J.A., Liao, J., Hong, Y., David Merryman, W., Wagner, W.R., and Sacks, M.S. Tissue-to-cellular level deformation coupling in cell micro-integrated elastomeric scaffolds. Biomaterials **29,** 3228, 2008.
108. Mathew, G., Hong, J.P., Rhee, J.M., Leo, D.J., and Nah, C. Preparation and anisotropic mechanical behavior of highly-oriented electrospun poly(butylene terephthalate) fibers. J Appl Polym Sci **101,** 2017, 2006.
109. Nerurkar, N.L., Baker, B.M., Chen, C.Y., Elliott, D.M., and Mauck, R.L. Engineering of fiber-reinforced tissue with anisotropic biodegradable nanofibrous scaffolds. Transactions of 28th Annual IEEE-EMBS Meeting, 2006, pp. 787–790.
110. Klouda, L., Vaz, C.M., Mol, A., Baaijens, F.P., and Bouten, C.V. Effect of biomimetic conditions on mechanical and structural integrity of PGA/P4HB and electrospun PCL scaffolds. J Mater Sci Mater Med **19,** 1137, 2008.
111. De Vita, R., Leo, D.J., Woo, K.D., and Nah, C. A constitutive law for poly(butylene terephthalate) nanofibers mats. J Appl Polym Sci **102,** 5280, 2006.
112. Nerurkar, N.L., Mauck, R.L., and Elliott, D.M. ISSLS prize winner: Integrating theoretical and experimental methods for functional tissue engineering of the annulus fibrosus. Spine **33,** 2691, 2008.
113. West, J.R., Juncosa, N., Galloway, M.T., Boivin, G.P., and Butler, D.L. Characterization of *in vivo* Achilles tendon forces in rabbits during treadmill locomotion at varying speeds and inclinations. J Biomech **37,** 1647, 2004.
114. Mauck, R.L., Yuan, X., and Tuan, R.S. Chondrogenic differentiation and functional maturation of bovine mesenchymal stem cells in long-term agarose culture. Osteoarthritis Cartilage **14,** 179, 2006.
115. Skaggs, D.L., Weidenbaum, M., Iatridis, J.C., Ratcliffe, A., and Mow, V.C. Regional variation in tensile properties and biochemical composition of the human lumbar anulus fibrosus. Spine **19,** 1310, 1994.
116. Pham, Q.P., Sharma, U., and Mikos, A.G. Electrospun poly(epsilon-caprolactone) microfiber and multilayer nanofiber/microfiber scaffolds: characterization of scaffolds and measurement of cellular infiltration. Biomacromolecules **7,** 2796, 2006.
117. Chao, P.H.G., Roy, R., Mauck, R.L., Liu, W., Valhmu, W.B., and Hung, C.T. Chondrocyte translocation response to direct current electric fields. J Biomech Eng Trans Asme **122,** 261, 2000.
118. Stankus, J.J., Guan, J., Fujimoto, K., and Wagner, W.R. Microintegrating smooth muscle cells into a biodegradable, elastomeric fiber matrix. Biomaterials **27,** 735, 2006.
119. Telemeco, T.A., Ayres, C., Bowlin, G.L., Wnek, G.E., Boland, E.D., Cohen, N., Baumgarten, C.M., Mathews, J., and Simpson, D.G. Regulation of cellular infiltration into tissue engineering scaffolds composed of submicron diameter fibrils produced by electrospinning. Acta Biomater **1,** 377, 2005.
120. van Tienen, T.G., Heijkants, R.G., Buma, P., de Groot, J.H., Pennings, A.J., and Veth, R.P. Tissue ingrowth and degradation of two biodegradable porous polymers with different porosities and pore sizes. Biomaterials **23,** 1731, 2002.
121. Nam, J., Huang, Y., Agarwal, S., and Lannutti, J. Improved cellular infiltration in electrospun fiber via engineered porosity. Tissue Eng **13,** 2249, 2007.
122. Simonet, M., Schneider, O.D., Neuenschwander, P., and Stark, W.J. Ultraporous 3D polymer meshes by low-temperature electrospinning: use of ice crystals as a removable void template. Polym Eng Sci **47,** 2020, 2007.
123. Balguid, A., Mol, A., van Marion, M.H., Bank, R.A., Bouten, C.V., and Baaijens, F.P. Tailoring fiber diameter in electrospun poly(epsilon-caprolactone) scaffolds for optimal cellular infiltration in cardiovascular tissue engineering. Tissue Eng Part A 2009 (in press, available online PMID: 18694294).
124. Janjanin, S., Li, W.J., Morgan, M.T., Shanti, R.M., and Tuan, R.S. Mold-shaped, nanofiber scaffold-based cartilage engineering using human mesenchymal stem cells and bioreactor. J Surg Res **149,** 47, 2008.
125. Nesti, L.J., Li, W.J., Shanti, R.M., Jiang, Y.J., Jackson, W., Freedman, B.A., Kuklo, T.R., Giuliani, J.R., and Tuan, R.S. Intervertebral disc tissue engineering using a novel hyaluronic acid-nanofibrous scaffold (HANFS) amalgam. Tissue Eng Part A **14,** 1527, 2008.
126. Inanc, B., Arslan, Y.E., Seker, S., Elcin, A.E., and Elcin, Y.M. Periodontal ligament cellular structures engineered with electrospun poly(DL-lactide-co-glycolide) nanofibrous membrane scaffolds. J Biomed Mater Res A 2009 (in press, available online, PMID: 18491392).
127. Baker, B.M., Gee, A.O., Jennings, M.W., Nathan, A.S., Huffman, G.R., and Mauck, R.L. Engineering anatomically-

shaped meniscus constructs: biologic and mechanical integration. Trans Orthop Res Soc **33,** 1460, 2008.
128. Nerurkar, N.L., Orlansky, A.S., Sen, S., Elliott, D.M., and Mauck, R.L. Multiscale tissue engineering of the intervertebral disc. Trans Orthop Res Soc **33,** 340, 2008.
129. Hong, Y., Fujimoto, K., Hashizume, R., Guan, J., Stankus, J.J., Tobita, K., and Wagner, W.R. Generating elastic, biodegradable polyurethane/poly(lactide-co-glycolide) fibrous sheets with controlled antibiotic release via two-stream electrospinning. Biomacromolecules **9,** 1200, 2008.
130. Verreck, G., Chun, I., Peeters, J., Rosenblatt, J., and Brewster, M.E. Preparation and characterization of nanofibers containing amorphous drug dispersions generated by electrostatic spinning. Pharm Res **20,** 810, 2003.
131. Brewster, M.E., Verreck, G., Chun, I., Rosenblatt, J., Mensch, J., Van Dijck, A., Noppe, M., Arien, A., Bruining, M., and Peeters, J. The use of polymer-based electrospun nanofibers containing amorphous drug dispersions for the delivery of poorly water-soluble pharmaceuticals. Pharmazie **59,** 387, 2004.
132. Li, W.J., Jiang, Y.J., and Tuan, R.S. Cell-nanofiber-based cartilage tissue engineering using improved cell seeding, growth factor, and bioreactor technologies. Tissue Eng Part A **14,** 639, 2008.
133. Lee, C.H., Shin, H.J., Cho, I.H., Kang, Y.M., Kim, I.A., Park, K.D., and Shin, J.W. Nanofiber alignment and direction of mechanical strain affect the ECM production of human ACL fibroblast. Biomaterials **26,** 1261, 2005.
134. Moffat, K.L., Kwei, A.S., Spalazzi, J.P., Doty, S.B., Levine, W.N., and Lu, H.H. Novel nanofiber-based scaffold for rotator cuff repair and augmentation. Tissue Eng Part A **15,** 115, 2009.
135. Song, J.H., Kim, H.E., and Kim, H.W. Electrospun fibrous web of collagen-apatite precipitated nanocomposite for bone regeneration. J Mater Sci Mater Med **19,** 2925, 2008.
136. Li, W.J., Chiang, H., Kuo, T.F., Lee, H.S., Jiang, C.C., and Tuan, R.S. Evaluation of articular cartilage repair using biodegradable nanofibrous scaffolds in a swine model: a pilot study. J Tissue Eng Regen Med **3,** 1, 2009.
137. Provenzano, P.P., Hayashi, K., Kunz, D.N., Markel, M.D., and Vanderby, R., Jr. Healing of subfailure ligament injury: comparison between immature and mature ligaments in a rat model. J Orthop Res **20,** 975, 2002.
138. Iatridis, J.C., and ap Gwynn, I. Mechanisms for mechanical damage in the intervertebral disc annulus fibrosus. J Biomech **37,** 1165, 2004.
139. Petersen, W., and Tillmann, B. Collagenous fibril texture of the human knee joint menisci. Anat Embryol (Berl) **197,** 317, 1998.
140. Pedicini, A., and Farris, R.J. Mechanical behavior of electrospun polyurethane. Polymer **44,** 6857, 2003.
141. Stankus, J.J., Guan, J.J., and Wagner, W.R. Fabrication of biodegradable elastomeric scaffolds with sub-micron morphologies. J Biomed Mater Res A **70A,** 603, 2004.
142. Rockwood, D.N., Woodhouse, K.A., Fromstein, J.D., Chase, D.B., and Rabolt, J.F. Characterization of biodegradable polyurethane microfibers for tissue engineering. J Biomater Sci Polym Ed **18,** 743, 2007.
143. Bhattarai, S.R., Bhattarai, N., Yi, H.K., Hwang, P.H., Cha, D.I., and Kim, H.Y. Novel biodegradable electrospun membrane: scaffold for tissue engineering. Biomaterials **25,** 2595, 2004.
144. Jin, H.J., Chen, J., Karageorgiou, V., Altman, G.H., and Kaplan, D.L. Human bone marrow stromal cell responses on electrospun silk fibroin mats. Biomaterials **25,** 1039, 2004.
145. Huang, L., Nagapudi, K., Apkarian, R.P., and Chaikof, E.L. Engineered collagen-PEO nanofibers and fabrics. J Biomater Sci Polym Ed **12,** 979, 2001.
146. Jiang, H.L., Fang, D.F., Hsiao, B.J., Chu, B.J., and Chen, W.L. Preparation and characterization of ibuprofen-loaded poly(lactide-co-glycolide)/poly(ethylene glycol)-g-chitosan electrospun membranes. J Biomater Sci Polym Ed **15,** 279, 2004.
147. Lee, K.H., Kim, H.Y., Khil, M.S., Ra, Y.M., and Lee, D.R. Characterization of nano-structured poly(epsilon-caprolactone) nonwoven mats via electrospinning. Polymer **44,** 1287, 2003.

Address reprint requests to:
Robert L. Mauck, Ph.D.
McKay Orthopaedic Research Laboratory
Department of Orthopaedic Surgery
University of Pennsylvania
36th St. and Hamilton Walk
Philadelphia, PA 19104

E-mail: lemauck@mail.med.upenn.edu

Received: November 27, 2008
Accepted: February 10, 2009
Online Publication Date: April 10, 2009